AN INVESTIGATION OF BODY WAVE MAGNITUDE USING THE NEW DIGITAL SEISMIC RESEARCH OBSERVATORIES PLUS CONVENTIONAL CATALOGUE DATA

by

JANET CATHERINE JOHNSTON PRUSZENSKI

B.S. Massachusetts Institute of Technology (Physics) (1976)
B.S. Massachusetts Institute of Technology (Earth and Planetary Sciences) (1976)

SUBMITTED IN
PARTIAL FULFILLMENT
OF THE REQUIREMENTS FOR THE
DEGREE OF MASTER OF SCIENCE

at the

MASSACHUSETTS INSTITUTE OF TECHNOLOGY

September 1979

Signature of Author.....

Department of Earth and Planetary Sciences, September 1, 1979

Certified by.....
Thesis Supervisor

Accepted by.....
Chairman, Departmental Committee on Graduate Stude

WITHDRAWN
MASSACHUSETTS INSTITUTE OF TECHNOLOGY
FROM
SEP 17 1979
MIT LIBRARIES
LIBRARIES

AN INVESTIGATION OF BODY WAVE MAGNITUDE USING THE NEW DIGITAL SEISMIC RESEARCH OBSERVATORIES PLUS CONVENTIONAL CATALOGUE DATA

by

JANET CATHERINE JOHNSTON PRUSZENSKI

Submitted to
the Department of Earth and Planetary Sciences
on August 10, 1979, in partial fulfillment of the requirements
for the Degree of Master of Science

ABSTRACT

Body wave magnitude is examined: how it is measured and factors affecting its calculation. Bias, a correction to log A/T in addition to the standard amplitude-distance curves, is illustrated using data from the International Seismological Center catalogue. It is shown that biases determined from these data are questionable. For the purpose of determining accurate biases, preliminary data from the new, digital Seismic Research Observatories are examined. It was found that the average digital network's m_b values were close to the m_b's reported by conventional stations. It is shown, however, that a source to station bias of up to 1.0 magnitude units can exist between a station pair.

Thesis supervisors:

Dr.M.A.Chinnery,Senior research associate
Dr.M.N.Toksöz,Professor of geophysics

Part 1

I. Introduction

The shape of a short period seismogram is the product of the characteristics of the source, and of the receiver, and the entire ray path. There are basically three places along the path that influence the resulting seismogram most, these are the lower mantle where the ray bottoms, the upper mantle and crust beneath the source, and the upper mantle and crust beneath the receiver. It has been shown from travel time and amplitude studies that inhomogeneities do exist at depth along P-ray paths under such large features as Hawaii (Kanasewich and Gutowski, 1975), the Caribbean Sea (Jordon and Lynn, 1974) and other areas (Toksöz and Sengupta, 1977). It has, however, been difficult to fix the depth. It has also been shown that inhomogeneities exist in the upper mantle (Aki, 1977, and many others). As a result of this, attenuation tables of body wave amplitude with distance must be corrected for accurate m_b estimates. Studies of these correction factors have been made (usually ascribing the correction to either the source or receiver) using existing catalogue data (Chinnery, 1979). It has been shown (Chinnery, 1978), using magnitude-frequency statistics, that this type of data is inadequate because of variable station factors resulting in inconsistent m_b reports (see part 1, section IV). Therefore, it is not known how large biases can be. Also these correction

factors may change very fast with source region location (Sengupta, 1975). How to calculate bias is also a problem. Various methods are assessed in section III (part 1). In order to eliminate the inconsistencies of the non-digital networks, preliminary data from the (A)SRO's is examined.

The new (A)SRO stations should not suffer from the inconsistencies of the non-digital network; they are well calibrated and their digital waveforms are readily available to the analyst for personal reading. Because of this accuracy conclusions may be drawn from even a small dataset. It should be possible to improve m_b calculations by using these stations in conjunction with the non-digital network.

In this thesis we discuss the magnitude bias problem in some detail (section II, part 1) and we consider the effects of clipping and receiver bias on non-digital stations (section IV, part 1). In order to demonstrate the size of amplitude attenuation correction factors, data from two digital stations, Kabul and Mashed are analyzed in some detail (part 2).

II. The Importance of m_b

m_b is calculated from the formula:

$$m_b = \log A/T + Q$$

where A is the amplitude of the P wave arrival, Q is the correction for attenuation with distance, and T is the period of the arrival (T ranges from 0.5 sec to a few seconds for body waves).

There are several reasons why we wish to determine body wave magnitude accurately. Most of them are interrelated. One major reason is that m_b combined with M_s (T = 20 sec) for an event gives us information on the spectra of seismic waves (see Aki 1972 and 1967) generated by earthquakes.

Another area of interest is seismic risk. There are many parameters of earthquakes that are often quoted as measurements of earthquake size. A few of these are maximum epicentral intensity, radiated seismic energy, body wave magnitude m_b, surface wave magnitude M_s, and seismic moment M_o. The last three are most commonly quoted for earthquake size. It is not clear that any one parameter can represent the true size of an earthquake because different disciplines are interested in different aspects of "size."

The moment of an earthquake is related to the physical dimensions. It is directly related to the rupture length l, the rupture width w, the amount of slip D, and the rigidity modulus μ by the formula:

M_o = lwD (Kanamori and Anderson, 1975) (2)

Although moments can be determined from seismograms through a fairly simple amplitude spectrum analysis, relative to magnitude, less moments have been calculated and those are mostly for large earthquakes. Since so few moments have been calculated, a relationship between moment and magnitude (the most readily available measurement) is desirable. Chinnery and North (1975) demonstrated that a nonlinear relationship exists between M_S and moment. This conclusion was dependent, however, on the reliability of the magnitude data used. They found a linear M_S-moment relationship for M_S less than about 7.0 and a departure from linearity trending towards the vertical near M_S = 8.6 (see Figure 1). If correct, this means that, while the moments of earthquakes may increase without bound (subject to physical constraints), corresponding M_S values will nonetheless have an upper limit. This seems logical for the following reason. The propagation time of a dislocation along a fault for a large earthquake (fault length greater than 100 km) may be larger than the 20 sec period at which we measure the spectral amplitude. This would result in a lower M_S. The general shape of the spectrum of seismic waves is usually flat at the lower frequency end and falls off rapidly after a "corner frequency" (many references, see Aki 1967 for example). The corner frequency is a function of the earthquake dimensions and occurs at

lower frequencies as the size of the earthquake increases. If for a particular event, the corner frequency is lower than that frequency corresponding to the 20 sec M_s period, then the amplitude at 20 sec will not reflect the larger size of the event in a linear way, and M_s will be lower than expected. A very important question is whether such a non-linear relationship exists for body wave magnitude. This question is not addressed here. If body wave magnitude and seismic moment are not linearly related, a single amplitude measurement on the first arrival may represent only a fraction of the energy radiated at 1 sec and m_b should not be used to assess seismic risk.

When we are examining long-term phenomena, we are limited to about 10-15 years of conventionally instrumented magnitude data plus 50 or 60 years of highly questionable data. While the most meaningful existing single parameter of earthquake size may be the moment, unless half a century of data is to be disregarded, we must utilize the magnitude scale. It may be that we shall have to abandon all this data because of problems with magnitude calculations from seismic networks, poor quality seismograms, and possible saturation of body wave magnitude with moment at high m_b's.

III. Factors That Affect m_b

A. Log A/T

i) Minimum detection thresholds.

At any recording station, the minimum detectable amplitude should depend on the noise level at the station. At nondigital stations, the minimum detectable signal will also be a function of the station magnification. At the digital stations, event detectors on the short period instruments are not adjusted to record such small amplitudes (see North, 1978). North found that many (A)SRO stations had a 50% detection cutoff at approximately $m_b = 4.5$.*

ii) Clipping at large amplitudes.

For non-digital stations a best-case scenario is when only mechanical clipping occurs, i.e., the trace overshoots the seismogram paper. This would prevent the operator from reading the amplitudes. This is discussed in detail in Section IV.

A more realistic case is that operators may have difficulty measuring traces that are large. This is demonstrated in Section IV to be a highly variable factor. It may be a function of the noise at the station during the arrival and of changes in personnel reading amplitudes.

---

*These stations were CMTO, KAAO, MAIO and ANMO. Probabilities were computed by coincidence of recorded time periods with theoretical arrival times for SCAC events.

If one assumes a shape for the true frequency-magnitude curve sampled by a station, then a reporting probability curve for that station can be described completely by five parameters (see Figure 2). These are G_D and G_S, the 50% detection and saturation thresholds respectively, γ_D and γ_S, a measure of the spread of the detection and saturation curves (the integral of the Gaussian function was used to approximate the falloff at both ends), and P_r, the maximum reporting probability (P_r is actually never equal to 100% for many reasons, such as station down time or instrument failure. A method for computing P_r for the events of interest at a particular station must be determined). The flat section, which theoretically reports with a probability close to 1.0, may be wide or just a point, or detection and saturation falloffs can intersect leaving no linear range.

To summarize, under ideal conditions (see Section IV) the shape of an individual station's frequency-magnitude curve should be the product of the reporting probability curve (adjusted for bias--see Section III.c) and the true frequency magnitude curve of the seismicity sampled by that station.

B. Q-factors*

Q-factors (which are actually amplitude-distance corrections) were determined for the purpose of relating observations of A and T at a remote station to the source characteristics. A standard shock was chosen and its surface wave amplitude at a given distance fixed the zero level.

---

*not to be confused with the attenuation parameter.

Richter (1958) determined the amplitude - distance correction for body waves using events whose surface wave magnitudes had already been determined. He later revised these factors for use with deep events. Revised versions of these curves (Gutenberg and Richter, 1956) are used today for source-receiver combinations over the entire globe. There is evidence that this is reasonable if the curves are considered to be only approximate estimates of attenuation on a global basis. Carpenter et al. (1967) obtained amplitude-distance curves independently (from the explosions in various test sites) which agreed well with Richter's results. (Explosions hold the benefit of having isotropic radiation patterns.) All data used in extracting magnitude correction factors are very scattered with values of log A often spanning one magnitude unit.

A more recent investigation was carried out by Sengupta and Toksöz (1977). They used only deep focus events in their amplitude study in order to eliminate at least one source of inhomogeneity (the lithosphere beneath the source). Their data agreed best with Carpenter's for short period.

To summarize, there are at least two sources of error introduced to magnitudes by the amplitude-distance corrections. These are: 1) departures of the Gutenberg and Richter curve from a true global mean; 2) departures from the global mean for a particular source-receiver pair (path dependence).

C. Station Bias

We will define bias as a correction to body wave magnitude, in addition to the standard amplitude-distance curves discussed above. Bias can be a function of the source or receiver location or both. Whether to incorporate scattering effects into bias is a complex problem (see section D, below). If scattering is a random process it should not be included in bias. We will consider bias to include only: 1) regional variations in the standard amplitude -distance curves (ray path dependence); 2) near source effects; 3) near receiver effects. We will exclude from "bias": 1) scattering effects; 2) measurement errors 3) radiation patterns. Figure 3 shows for 9 stations the result of subtracting from an individual station the average m_b reported for an event. These events are from the International Seismological Center catalogue from 1964 to 1973. Only events that were within 21° to 100° of 15 or more stations that reported an m_b were used. The numbers given are the number of events in the sample and the mean and standard deviation of the sample (from North, 1977). The striking feature is the similarity in shape for all the 9 stations, suggesting that some of the curves are shifted to the left or right by some kind of bias effect. There is other evidence for the existence of bias. For example, in a comparison of m_b's assigned by PDE (Preliminary Determination of Epicenters) and Russian sources, it was found that

Russian magnitudes were larger. This was apparently because PDE used stations in the western United States which consistently reported lower m_b's than the rest of the stations (Brune et al., 1970).

The amplitude and period of a P-arrival will always represent the combined attenuation effects of the source region, the ray path and the station region. To isolate which of these regions is most responsible for biasing m_b is very difficult. It has been demonstrated that large variations in Q do exist in the upper mantle (Solomon and Toksöz, 1970; Molnar and Oliver, 1969; Khalturin et al., 1976; Romanowitcz, 1978). It appears that a low Q is well correlated with high heat flow (Romney et al., 1962; Evernden and Clark, 1970) and with certain geotectonic structures such as tectonic zones and oceanic ridges. (Attentuation seems to be highest in the regions of mid-ocean ridges, concave sides of island arcs and rift structures). See North (1977) for additional references.

Even if bias is isolated to the source or the receiver region, it may be sensitive to the distance between them and therefore to the angle of incidence and emergence. It may also be sensitive to the azimuth depending upon the symmetry of the attenuation medium. If spherical symmetry is assumed, then for a given event the source contribution to the bias for a single event will be the same at all the stations and the variation in m_b across a network would be the result of a different station bias and/or ray path bias.

To explore further the difficulties involved in calculating biases two methods will be described. The first method, used by North (1977), associates a bias with a particular station. He determined global biases for 72 stations that were chosen because of their frequency of reporting in the ISC catalogue for 1964 to 1973. Bias was computed by the formula:

$$b_{ij} = m_{ij} - m_j \qquad (3)$$

where b_{ij} is the bias at the i^{th} station for the j^{th} event and m_j is the network average m_b with at least 15 of the 72 stations reporting an m_b and m_{ij} is the station magnitude. Standard deviations of the mean were computed and found to be rather large (0.35 m_b units). Explanations given for this are: temporal changes in station bias, dependence of bias on source region, and possible dependence of bias on event magnitude. North did find mean bias variations with time (see Figure 4) for a few stations and had no explanation for this. Table 2 shows his results for stations in various geographical regions for different sources. Numbers reported are the deviation of bias for a source region from a global mean bias. It can be seen that, for a given receiver location, biases change with source region, and for a given region biases change with receiver location, (with the possible exception of region 4, Japan to U.S. station). Variations with magnitude seemed to be small. He concluded that his biases were an effect of attenuation in

the region near the seismic stations and assigned certain global baises to his 72 station network. These biases correlated very well with geotectonic settings (for example, biases were mostly negative for the western U.S. and positive for the eastern U.S.).

A second method for computing a magnitude bias is described in a paper by J. Vanek et al. (1976). They define some "homogeneous" network of stations and compute biases for these stations for many observations relative to just one reference station. The requirement for being a suitable reference station was insensitivity to a regional effect. Although not explicitly stated the biases computed seemed to be for use at a particular source region. All the stations in the network were close to each other.

There are major drawbacks in each of these methods. This first method assumes the existence of a global bias for a station. Biases are shown to vary with source region, but a global bias assumes differences will average out in a large data set. This may not be true since stations sample different areas and distributions of seismicity. The method also fails to adequately define "zero bias." For every event, no matter which 15 or more network stations reported m_b's, they, along with the station whose bias is computed, are averaged together for an m_b of zero bias. Different source regions will have a different network of stations in range. These stations may have a net bias high or low with respect to a set of stations in range of another source

region. Also, not all the stations were in operation for the time period considered. Another problem is in the definiton of "good" stations as those which reported frequently. Stations that report infrequently may do so because they have low magnifications. This might enhance their ability to report large m_b events, and therefore valuable information is excluded if they are not incorporated into the bias calculations.

The second method also has problems defining zero bias. Using just one reference station can be dangerous unless a very large data base is available (scattering problems, see Section III.D). Since the biases were computed for stations very close together, it may not be possible to use these stations in conjunction with other networks. Neither method addresses the problem of how quickly bias changes with source location. All the source areas are very large. An attempt to map bias at a station for segments along an island arc for example would be interesting.

In fairness to the authors of the previously mentioned papers, it must be emphasized that a large data base must be used if any numerical biases are to be extracted. Every restriction placed on the data drastically reduces the number of events that meet all the requirements.

D. Scattering

A true magnitude m is related to the above parameters and scattering by the formula:

$$m + \varepsilon = \log A/T + Q + B$$

where ε is the scattering parameter,* and B is the bias.

Estimates of scattering are usually made from variations of m_b across a network of stations for a given set of events. (Von Seggern, 1973, Evernden and Clark, 1970). This method actually includes the effects of scattering plus bias (ε and B above), and when these variations are modelled as a random Gaussian phenomenon, with a zero mean, a standard deviation of approximately 0.3 is obtained (see Chinnery 1978 and von Seggern 1973).

Aki (1973) interpreted variations in P amplitude across the LASA (Large Aperture Seismic Array) as being the result of scattering by <u>random</u> inhomogeneity in the crust beneath the array. If scattering is a random effect it should be possible to separate it from the bias effect, which is certainly non-random.

---

*Scattering is the term used to describe diffraction effects on seismic waves caused by small scale inhomogeneities along the ray path (see Bullen, 1965, p. 71).

IV. Ideal Networks vs. ISC Catalogue Data

An ideal network of stations, operating in a homogeneous planet, will report for an event of true magnitude m, that magnitude to within a statistical error regardless of the locations of the individual stations or the location of the event. To date, no such network exists. Now if we allow inhomogeneities in the earth, we will introduce biases. Consider three sections of the ray path: the crust and upper mantle near the source and near the receiver, and where the ray bottoms. A ray in the 30° to 90° distance range bottoms between 1000 and ∿2700 km. Since inhomogeneities at this depth are not well documented, let us consider bias to be a local effect of either the source or the receiver or both. Now, if we had a station surrounded by events of known magnitude, and the bias for each event were significantly different, then bias could be located to the source region. Similarly, if we had an event, surrounded by stations that each reported different biases, the bias would be a function of receiver location. The effect of bias combined with the existence of minimum and maximum detection cutoffs is very important in magnitude calculations. A catalogue report of m_b is generally the result of averaging several stations' reported values. If the true m_b is in the linear operating range of each station, this technique is reasonable if it is assumed that the net bias of the set of stations is zero. If our m_b is large, then the stations

that have a high positive bias may be clipped and not report at all, thus biasing the average m_b low. The opposite effect occurs for low m_b's, so that conventional catalogue m_b reports underestimate larger earthquakes and overestimate smaller earthquakes.

For an ideal network, we would like to know when an event is "not seen" by a particular station whether it was not reported because it was too small or too large, or because the station was not in operation at the time. If it were too small, it would be desirable to have the noise level reported. Once the reporting probability parameters are determined for all the stations in the network and bias is added, one can compute the "expected value" of a station's reported m_b, given an event of true m_b (see Ringdal, 1975). A detailed statistical model, which uses a minimum detection cutoff only, can be found in references (Christofferson et al., 1975) and will not be repeated here.

Figure 5 outlines schematically a possible procedure for computing m_b. The first steps are concerned with the setup of a network. Selecting a set of stations will be a function of the sampling area chosen and vice-versa. A global or small region in range of all the stations may be chosen. Ideally some overlap in station ranges is desirable as is having isotropic distribution of events about any station. Once stations have been selected, reporting probability parameters should be estimated for them. Next, a set of events from the sampling area must be chosen. The choices are: 1) the set of events seen by all the stations; 2) the set of events

seen by at least N stations (where N is some integer less that the total number of stations); 3) the set of events seen by N' particular stations every time (where N' is some number that is large enough to cancel scattering effects). Step 5 is to record reported m_b and reports of "not seen" for all events for all stations (within a certain range--30° to 90° for example). Before many reports for a given event can be combined, the stations' biases must be computed.

Once biases have been determined, one can then compute average magnitudes for all events either by simply adding biases to individual station reports or by combining bias estimates with reported "not seen" information and statistically estimating an m_b for stations not reporting and then averaging the station magnitudes. This procedure should produce a consistent magnitude estimate.

We have assumed in this ideal network that:

a. Reporting probability parameters can be determined;

b. All of the stations are in range of a large enough number of common events so that biases can be determined;

c. Our reference station(s) are in range of and report many of these events;

d. Failure to report is the result only of instrumental sensitivity and not operator incompetence or station downtime;

e. There are no large variations of bias with time;

f. Additional ideal factors exist, such as strict and frequent calibration of recording instruments.

A study of station reporting probability parameters using ISC body wave magnitude data was made (Chinnery, 1978) for long-time intervals. The stations used were a subset of those for which North (1977) had calculated biases. For a given station over a selected time period, plots of m_b vs. log N (number of events) were generated. One plot of m_b vs. log N is shown in Figure 6. The rise of detection probability can clearly be seen as can a fall-off in detection at high magnitudes. Only events in the 30° to 90° range were used. A linear frequency magnitude relationship was fit to the apparent linear section (between 5.2 and 6.3) and probability reporting parameters were read off. This technique proved unsatisfactory when it was found that different stations had different slopes for their "linear" sections. To discount variations in sampled seismicity as the cause, a test region, the Aleutians-Kurils area was used for all the stations in range of it.

A surprising result was that although the shape of most stations' curves for this area varied the VELA arrays in the western U.S., all had the same shape which was very different from the other stations. Figure 7 shows data from 3 of these stations, UBO , TFO, BMO. These stations all show a

frequency-magnitude relationship that is linear (with slope $\sim$ 0.9) up to m_b = 5.8, and then curve downward, becoming vertical between m_b=7.0 to 7.5. To contrast this, Figure 8 shows a 25-station network average for the test region with the VELA arrays omitted. The curve drawn in is the VELA seismicity curve discussed above. The stations in the network are listed in Table I. The two curves are clearly inconsistent, showing an overshoot in the 5.0 to 5.7 range and an undershoot in the higher m_b's. Obviously, both the VELA stations and the 25-station network cannot be reporting true seismicity. The possibilities are either that one network is reporting accurately or neither are. Most probably the VELA array stations are the closest to being accurate. They have well-trained operators, a large linear operating range and are carefully calibrated. In contrast, the other stations in the network seemed to change their reporting probabilities from year to year. This was presumed to be a manifestation of a change in operator or a change in magnification. A study of how station magnification might be related to reporting probability parameters was made. The simplistic assumption was that an operator would only report an amplitude and a period for a trace if both the peaks were not clipped. In this way, a peak-to-peak amplitude that was one-half the size of the page would be assigned a probability of 50% and so on. Table II lists some reporting probabilities calculated for various popular magnifications. When compared with the network stations

described above, a few stations' log A/T curves appeared to follow the clipping curve. Figure 9 shows such a station, SJG, in Puerto Rico for the period 1965 to 1971 ($30 \leq \Delta \leq 90$). Although the extent of agreement is, of course, contingent on the assumed frequency magnitude distribution, it is reasonable to assume some linear seismicity curve roughly parallel to the $1.8 \leq \log A/T \leq 2.5$ segment of the curve. The probability vs. log A/T curve was generated from amplitudes by assuming a period of 1 second always. The low end of the curve arbitrarily assigned a probability of 75% to an amplitude near the noise level of the seismograms. (This was very roughly estimated for SJG from looking at a few seismograms from that station). Unfortunately, the large majority of stations for which data and magnification factors were available showed a much lower cutoff than predicted by this model.

The conclusion from these studies is that the existing magnitude data from nondigital seismic stations are not reliable enough for any magnitude-frequency statistics. Most stations (not including the VELA array) have very small linear operating regions if they have any at all (there is a good possibility that these stations' detection and saturation curves overlap.) This is probably the result of erratic operator reporting. If this is true, then determining the real shape of the frequency-magnitude relationship from these stations is impossible.

PART 2 THE (A)SRO'S

I. Available Data

The (A)SRO's are new high quality seismic stations which record digital data. The SRO's are automatically calibrated every five days, and the ASRO's are calibrated by an operator at least once a month. Table III lists the station names and locations of (A)SRO's. Figure 10 is a map with the stations that had data recorded for the time period examined. These events were chosen from a preliminary listing in the Seismic Data Analysis Center Weekly Event Summary, from August 1977 to March 1978. Events listed with an m_b of 4.5 or greater were chosen. Theoretical arrival times to the stations were calculated, and those times were extracted from the (A)SRO digital data when available (the [A]SRO's have an automatic event detector, so if there is no data at a calculated arrival time, either the station was down or the event did not trigger the detector properly). Since new stations were put into operation each month, there was much more data available for the later months (i.e., August through December events would usually have 3 stations per event, whereas the later months could have 5 or 6). The stations that most frequently had data for events were ANMO, CHTO, GUMO, KAAO, MAIO, NWAO, TATO, CTAO, MAJO and ZOBO. Guam was malfunctioning during most of the events. It was found that the area of the Aleutians-Kurils had the largest number of events with a consistent network of stations.

Also, seismograms with a high background level of noise were discarded to avoid extensive filtering. The (A)SRO's have similar frequency response curves, and the amplitude correction as a function of period measured was applied (see Figure 11). The purpose of looking at this data was not to gather statistics on the network m_b's as has been done for the non-digital stations--there certainly is not enough data analyzed for m_b to do that--but to take advantage of the shape of the waveform in conjunction with the reported m_b. Many authors use catalogue reports of m_b assuming that the advantages of a large data base will outweigh the loss of accuracy from inconsistent reading of seismograms. This paper takes the opposite approach.

II. Error Estimates

Calibration of the (A)SRO's is supposed to be good to within 10% of the stated calibration. When the calibration was checked, however, some of the stations were high or low by more than 10%. (The SRO's send through a calibration pulse every 5 days; the ASROs' calibration must be checked indirectly.) To be safe, we estimated the calibration to be good to $\pm$20%. Actual measurement of amplitudes was fairly precise, to at least within 5%. Periods were measured to within $\pm$0.1 sec, which, when combined with the instrument correction and the amplitude error, introduced an absolute error of 0.2 into log A/T. A less straightforward source of the error is the Q-factor correction for attenuation with distance, which also depends on the depth. Although locations of events were accurate enough to not introduce errors from the Q-factor table, some of the listed depths were questionable. This would shift the computed value of m_b but would not affect the relative m_b's for one given event so severely since between 60° and 90° away (where most of the data lay) the Q-factor curve is its flatest (see Figure 12). Depths determined by finding a depth phase (as was the case for most of the events studied) were probably good to within 20 km, which translates into a maximum error in m_b of $\pm$0.2. Therefore, the total maximum possible error in m_b was about $\pm$0.4 magnitude units. If the two errors are considered to be random, the standard deviation in m_b

that results is less than 0.3 m_b units. When an m_b is considered relative to others computed in the network for the same event, the error is less because the depth error will roughly work in the same sense for all the stations. So when comparing m_b's around a network, an absolute error of ± 0.3 m_b units was assumed.

III. Results

A. m_b

m_b was calculated by two methods at first. The first arrival amplitude and the largest amplitude in the first four cycles were measured. The first method yielded m_b's that were smaller by roughly the same ratio across the network than the maximum amplitude m_b's (unless the first arrival coincided with the maximum amplitude). Because of the difficulty in identifying the first arrival in the case of noise at the station, the maximum amplitude method was used for all the data. With three or more ASRO's and SRO's per event, it was clear there was no gross discrepancy in m_b between these stations and the bulletin listed m_b. Figure 13 shows a histogram of the difference of the listed m_b for an event and the ASRO-SRO network average. For 24 stations, and depth $\leq$ 100 km, the average difference is zero with a root mean square difference of.3. This is certainly reasonable considering the small size of the network (3 or 4 stations usually) and scattering effects. The listed m_b was usually calculated from approximately 10 stations.

It was observed that although the SRO's short period instruments peak at approximately 0.4 sec, most of the measured periods were greater than 1.0 sec. So far the only explanation for this is the attenuation of the higher frequencies with distance.

The distribution of magnitudes across the network was examined for the Aleutians, the area that had the most

events for the network. Figure 14 shows the two events' m_b's plotted. The data is from an event from the Fox Islands area and from the Andreanoff Islands. The listed depths are 57 km and 95 km respectively. There is fairly good coverage of these areas as can be seen in Figure 15, an azimuthal map centered at the Fox Island event. The striking feature of the distribution in Figure 14 is the large (nearly one) magnitude difference between Mashed and Kabul. Additional Aleutian data was plotted in Figure 16. Again the large difference between MAIO and KAAO is apparent.

Data plotted in Figure 17 from the Mid- and South-Indian rise regions do not show this tendency. How can the large difference between KAAO and MAIO in the Aleutian area be explained? It is convenient that the two extremes of the network are also the closest to each other in geographical location. Mashad is about 9° away from Kabul which translates into about 5° difference in the distance from an Aleutian Island event to the station. While the majority of the network's periods were over 1.0 sec, KAAO's periods were shorter.

B. Waveforms

So far the m_b data collected could all have come from a regular catalogue of non-digital stations (from which many more events would be available). The advantage of the (A)SRO Network is that we can look at the character of the waveforms in making an investigation of their computed m_b's.

For a given event waveforms recorded by short-period instruments across a network can vary greatly. Sometimes odd-looking waveforms are the results of a signal's superposition with noise. Figures 18a, 18b, 18c show 3 seismograms obtained for an event in Kamchatka. ANMO and CTAO are so noisy that one would hesitate to pick an A and T. KAAO, however, is very clear. When filtered with a high pass filter, with 6db point at 0.5 (corresponding to T = 2.0 sec), the shapes of the two seismograms agree much better with KAAO (Figures 18d, 18e). Note, however, the large difference in amplitude between ANMO and KAAO (both at approximately the same distance from the event). Possible explanations for this will be considered later.

An interesting occurrence is when the waveforms have the same messy shape (as in Figure 18a, 18b), but the noise level at the stations is very low. Figure 19 shows an example from the Kuril Islands. Here we have four stations, AMNO, CHTO, KAAO and MAIO, with near zero noise. Note particularly the similarity of CHTO and MAIO, both having similar waveforms and lower frequencies, contrasted with KAAO's high frequency content. One possibility for the shape of CHTO and ANMO is that a local event is occurring a few seconds into the arrival which is interfering. This seems unlikely because of the large separation of the two stations (Albuquerque, New Mexico, and Chang Mai, Thailand) and the similarity of their records. If there were another event in the source region, it should show up clearly in

KAAO's record, but this is not the case. It is also unlikely that the stations would pick up reflections from the surface at the station site; their burial depths do not exceed 100 meters, which is a very small fraction of a wavelength at that depth. Other possibilities at the source region are: starting and stopping phases resulting from a finite rupture velocity; pP interference from very shallow focus events; interference resulting from triplications in the travel time curve, and large scale inhomogeneity resulting from the subducting slab. The seismograms could easily be interpreted as showing a low energy start with a burst of large energy approximately 2 sec into the event.

Figure 20 shows a synthetic waveform with a Brune model P and inverted pP. As the pP-P delay time is shortened we see in Figures 21 and 22 increasing similarity to the data. (These synthetic seismograms use the same amplitude for pP and P.) In first analyzing this event it was decided that depending upon what was chosen as pP, the depth could be either less than 33 km of approximately 50 km (the listed depth is 47 km). Perhaps one can see a pP $\sim$2.0 sec into the KAAO waveform, and this event is really very shallow. This would introduce an error into any frequency-magnitude statistics but would not seriously effect variations in a network for single events as long as reasonable deltas were used.

Also, we must be aware that the introduction of pP amplitudes instead of P into our M_b calculations may affect

m_b in unpredictable ways. For example, when "clear" pP's were identified, sometimes their amplitudes were larger than P, sometimes smaller. A pP/P amplitude ratio will be highly sensitive to the attentuation coefficient of the path to the surface.

Another possibility is that multiple arrivals are occurring beneath the site. (P waves splitting up when striking geological structures beneath the receiver and arriving at slightly later times.) The similarity of the records from all the stations discounts this. For this particular event it seems likely that the character of recordings is a function mostly of the source, and somehow the high frequencies are "washed out" at all the stations except KAAO. One of the problems with magnitude measurements is the question of whether to measure the amplitude of the small onset, or the main burst of energy.

C. Discussion

So far we have not been able to account for the large differences in magnitude computed. Let us examine the extreme case, KAAO and MAIO, for some Aleutian Island events. Thirteen events from the Fox, Near, and Andreanoff Islands were analyzed. For these data, five events had seismograms from both KAAO and MAIO. For these five events the average difference between the two stations was 0.8 magnitude units with a standard deviation of 0.1. Figure 23 shows the network's records for two events in the Andreanoff Islands

and the Fox Islands. Note in the first event the higher frequency first arrival of KAAO's as compared to the other stations with the exception of MAIO. In the second event we again see more detail in KAAO's recording. The deltas in order for the first event are 51°, 79°, 76°, 79° and 35°; and 48°m 75°, 80° and 81° for the second event. The depths are listed as 95 km and 57 km. Additional data is shown in Figure 24 from the Kuril Islands. We will attempt to show that the difference in m_b reports between MAIO and KAIO is a result of a bias of one station with respect to the other caused by the geologic setting of the receivers. The absence of higher frequencies in MAIO relative to KAAO suggests immediately that the seismic waves that reach KAAO travel through a zone of lower attenuation than do those at MAIO. To check that the effects were not caused by a failing of the instrument, a few old events for which film chips were available for KBL and MSH (analogue stations situated near or at the same location as KAAO and MAIO) were examined. It was found that, although the frequency content of the signal was hard to assess on the old records, the amplitude difference was apparent and in the same sense as in the new digital stations.

The SRO at Mashad, Iran lies in the edge of the Binalud Mountains, a metamorphic chain with igneous intrusions. Rocks at the site location also appear to be intrusive according to the installation report. The drilling of the

borehole disclosed mainly andesite and basalt to a depth of 114 meters. Some short-period, low-amplitude noise was reported to be caused by a nearby rock quarry.

Canitez and Toksöz (1978) studied the structure of the Iranian plateau using dispersion and attenuation of Rayleigh waves from events recorded at Mashed and Shiraz. They found evidence for a high Q crust (600-1000) and a very low Q upper mantle (∿5-10) for shear waves. This region of low Q (depth = 65 to 95 km), they suggest, may be the result of heating of the lithosphere from below by convection induced before the collision of the Arabian plate with Iran. In the absence of compressional wave data, Q for shear waves is related to Q for p waves for the formula:

$$Q_\alpha^{-1} = \frac{4}{3}(\beta/\alpha)^2 \, Q_\beta^{-1}$$

(from Anderson et al., 1965). This highly attenuating medium may extend beneath and to the north of Mashed.

There was no installation report available for the ASRO at Kabul, Afghanistan; the geology near the site has been studied, however. Khalturin, Rautian, and Molnar (1976) studied P and S waves from intermediate depth earthquakes in the Pamir-Hindu Kush region recorded at stations in the vicinity of the earthquakes and to the north. They found relatively high frequencies at all the stations and inferred a relatively high Q (∿1000) for the ray paths. Figure 25, reproduced from their paper, shows the locations of the events they used. An event from the Aleutians or the Kurils

would pass through the zones marked by their events at an azimuth northeast of Kabul. The ray path to Mashad would miss the Hindu Kush area. A rough calculation demonstrates that the large bias of KAAO w.r.t. MAIO can be caused by a difference in Q over the ray paths. Using

$$A_i = A_o e^{-\pi f t_i^*}$$

where i is the station index, A_o is the non-attenuated amplitude, $t^* = t/Q$ (the travel time divided by Q), and f is the frequency of interest, we get for the amplitude ratio of Mashad to Kabul:

$$\frac{A_M}{A_K} = \frac{\exp[-\pi f t^*_M]}{\exp[-\pi f t^*_K]}$$

If it is assumed that the attenuation difference occurs over the last 60 km of path, the travel time for the Kabul path is 10 sec, and for Mashad is 12 sec, then for a period of T = 1 sec the amplitude ratio A_K/A_M is equal to 10, with $Q_M = 16$, $Q_K = 2000$.*

What about other azimuths? To contrast the Aleutian events, we looked 180° away in the same distance range, but there were few African events to choose from. The best that could be done was finding some events from the south (Mid- and Southeast-Indian Rises) and from the west (Crete). Figure 26 shows two events having listed m_b's of 4.7 and depths of 0 km. One is from the Mid-Indian Rise, the other

*This is a very extreme example, not meant as an actual model of the regions.

from the South-Indian Rise. In the first event we actually see more high frequency content at Mashad than at Kabul (their delta's are very close). Also, although Mashad is noisy, the amplitude at Mashad is clearly not an order of magnitude smaller than KAAO's. In the second event again, we see low attenuation of the higher frequencies at Mashad, and although both stations are noisy, it is again clear that Kabul's signal is not very much larger (there MAIO is 6° farther from the event than is KAAO).

Figure 27 shows two events from Crete. Both events show a lack of high frequency at KAAO, and the second event's amplitudes agree well (KAAO is 8° farther from the event). In the first event KAAO's amplitude would seem to be a bit high (the markers denote calculated P arrival times). There is, however, some sort of preceding activity starting ∿5 sec before the calculated P arrival. When overlaid with Mashad's seismogram, a much better fit was made by calling the onset of that low amplitude signal the P arrival. It was shown by Sheppard (1967) that amplitude variations were related to time residuals at stations. He found that a larger amplitude corresponded to an earlier arrival. Unfortunately, the range of time residuals he found were too small to be measured with the (A)SRO data because of the uncertainty of the location of events. If the arrival time of this event is really earlier than expected, it is probably because the onset of P was missed by many of the stations used to compute a latitude and longitude for the event.

If the amplitude "bias" of these two stations is caused by an attenuating medium about the stations, that attenuating medium is not symmetric. Therefore, any biases calculated for use with magnitude data from KAAO and MAIO will have to be calculated for source-receiver pairs.

IV. Discussion and Conclusions

When discussing a bias, it must be clearly stated how it has been calculated. This investigation clearly pointed to a relative bias of Kabul to Mashed (or vice-versa) for sources from the Aleutian Island region.

There are several factors that must be considered when trying to isolate the cause of this bias. Some of the major considerations are:

1. Subducting slab - if, from the Aleutians, the ray path to Kabul passes through the high Q subducted slab and the ray path to Mashed does not, this would increase the amplitude recorded at Kabul. Q-values of 1000 have been proposed for sinking slabs at island arcs (Le Pichon, et al., p. 242) whereas upper mantle values of 150 are typical.

It is unlikely, however, that this is occurring in our case. The subducting zone, as indicated by the seismicity, makes an angle of approximately 45° with the vertical. Rays traveling the distance to MAAO and KAAO from the Aleutians have a much steeper take-off angle ($\sim$23°). Both raypaths may indeed pass through the slab but this would affect both signals in the same manner.

2. Radiation Patterns - If Mashed were near a nodal plane and Kabul were not, this could easily produce the observed amplitude difference - with the number of (A)SRO's

operating at the time of this investigation an attempt to study radiation patterns was impractical. However, we note that the two stations plot in the upper left quadrant of a Schmidt net fault plane projection for an event in the center of the Aleutian Island arc (azimuth between 310° and 320°, takeoff angle between 20° to 25°). This position should not consistently place Mashed on a nodal plane (see Le Pichon, et al., p. 248).

3. Receivers - a) Mashed: It has been shown that there is a region of very low $Q(Q_\beta \approx 5\text{-}10)$ in a depth range of 65 to 95 km in a region (Canitez and Toksöz, 1978) between Shiraz and Mashed. An extension of this attenuating medium to the north of and under Mashed is consistent with the results of this study. b) Kabul: Khalturin et al. (1976) have observed the propagation of high frequencies and large amplitudes from events in the Hindu Kush area recorded at stations near the area. They suggest a relatively thick zone of high Q penetrating the asthenosphere as the cause. Such a zone, they hypothesize, might be caused by a remnant of previously subducted oceanic lithosphere, almost vertically oriented, cooling the surrounding asthenosphere. If it is as deep as is believed, a ray path to Kabul from the Aleutians would pass through this zone.

A quick calculation shows that this could account for a magnitude difference in amplitude. If we assume the difference in Q occurs over the last 500 km of the ray path, use an average Q along this section of 122 for Mashed and 2000 for Kabul, we get for the frequency of interest (1 Hz) an amplitude ratio of approximately 10 for Kabul for Mashed (see equation, section III C.).

Although hampered by the limited size of the data set during the time of this investigation, several conclusions can be drawn from this study. These are:

i) Relative biases between stations from a particular source region can be as large as one magnitude unit.

ii) If the relative bias of KAAO to MAIO is due to a difference of Q along the ray path, this difference is mostly occurring near the stations.

iii) If this difference in the attenuating medium is located near the stations, that medium is not symmetric about the stations.

iv) Biases must be computed for source-receiver pairs, or at least incorporate an azimuthal dependence about the stations.

How large a source region can be is a problem. This study suggests that a source region could be as large as the Aleutian Island arc. A travel time residual study with sources from the Aleutians would help define the

boundaries. Since travel time data is not as scattered or operator dependent as amplitude data, the nondigital stations, MSH, and KBL could be used (these have been in operation for a much longer time period and thus larger data base is available).

Currently, the new digital stations greatly increase our knowledge of earthquake magnitudes when used in conjunction with the other stations. In the future, when more of these stations are in operation, they may be used alone for a reliable and accurate seismic network.

ACKNOWLEDGEMENTS

I would like to thank Lincoln Laboratory for the use of their facilities along with Dr. Michael A. Chinnery, T. Fitch, R. Sheppard, P. Molnar and J. Nabelek for helpful discussion of the material and Ms. Leslie Turek for assistence in retrieving the digital waveforms from the data computer.

I would also like to thank M.N. Toksöz, K. Tubman, R. Stewart, A. Cheng , J. Pulli and S.C.Solomon for critical review of the manuscript.

This work was supported in part by my husband, Anthony S. Pruszenski, Jr., and by Lincoln Laboratory.

References*

Aki, K., Scaling law of seismic spectrum, J. Geophys. Res., 72, 1967.

Aki, K., Scaling law of earthquake source time function, Geophys. J.R. Astr. Soc., 31, 1972.

Aki, K., Determination of the three-dimensional seismic structure of the lithosphere, J. Geophys. Res., 82, 2, 1977.

Anderson, D.L., et al., Attenuation of seismic energy in the upper mantle, J. Geophys. Res., 70, 1965.

Bullen, K.E., The Earth's Density, Halstad Press, 1975.

Canitez, N., M.N. Toksöz, Rayleigh wave propagation and structure of the Iranian Plateau, unpublished manuscript, 1978.

Caputo, M., A mechanical model for the statistics of earthquakes, magnitude, moment and fault distribution, Bull. Seismol. Soc. Am., 67, 849-861, 1977.

Carpenter, E.W., et al., The amplitude-distance curve for short period teleseismic P-waves, Geophys. J. R. Astron. Soc., 1967.

Chinnery, M.A. and R.G. North, The frequency of very large earthquakes, Science, 190, 1197-1198, 1975.

Christoffersson, L.A., R.T. Lacoss, and M.A. Chinnery, Estimation of magnitude, Seismic Discrimination

*Additional references at the end of this section.

Semiannual Technical Summary, Lincoln Laboratory, M.I.T., December 1975.

Cosentino, P., V. Ficarra and D. Luzio, Truncated exponential frequency-magnitude relationship in earthquake statistics, Bull. Seismol. Soc. Am., 67, 1615-1623, 1977.

Fitch, T.J., and M.H. Worthington, Mechanisms of Australian earthquakes and contemporary stress in the Indian Ocean Plate, Earth Planet. Sci. Lett., 18, 345-356, 1973.

Frasier, C.W. and R.G. North, Evidence for ω-cube scaling from amplitudes and periods of the Rat Island Sequence (1965), Bull. Seism. Soc. Am., 68, 283-300, 1978.

Geller, R.J. and H. Kanamori, Magnitudes of great shallow earthquakes from 1904 to 1952, Bull. Seism. Soc. Am., 67, 587-598, 1977.

Gutenberg, B.C., and F. Richter, Magnitude and energy of earthquakes, Estratto da Annali di Geofisica, Vol. IX, 1, 1956.

Herrin, E., et al., 1968 Seismological tables for P phases, Bull. Seismol. Soc. Am., 58, 1193-1241, 1968.

Howell, B.F., Jr., Introduction to Geophysics, McGraw-Hill, New York, 1959.

Isenhour, W.R., Jr., Seismic Research Observatory, Final Installation Rpt., Mashad, Iran, UNITECH Inc., January 1976.

Jonas, F.B., L.T. Long, and J.H. McKee, Study of the

attenuation and azimuthal dependence of seismic-wave propagation in the southeastern United States, Bull. Seism. Soc. Am., 67, 1503-1513, 1977.

Jordan, T.H., W.S. Lynn, A velocity anomaly in the lower mantle, J. Geophys. Res., 79, 17, 1974.

Julian, B., M.K. Sengupta, Seismic travel time evidence for lateral inhomogeneity in the deep mantle, Nature, 242, 1973.

Kanamori, H., Quantification of earthquakes, Nature, 271, 411-414, 1978.

Kanamori, H., and P.C. Jennings, Determination of local magnitude M_1, from strong-motion accelerograms, Bull. Seism. Soc. Am., 68, 471-485, 1978.

Kanamori, H., and D. Anderson, Theoretical basis of some empirical relations in seismology, Bull. Seism. Soc. Am., 65, 5, 1975.

Kanasewich, E.R., P.R. Gutowski, Detailed seismic analysis of a lateral mantle inhomogeneity, Earth Planet. Lett., 25, 1975.

Khalturin, V.I., T.G. Rautian, and P. Molnar, The spectral content of Pamir-Hindu Kush intermediate depth earthquakes; evidence for a high Q zone in the upper mantle, J. Geophys. Res., 1976.

Marshall, P.D., D.L. Springer, Is the velocity of Pn an indicator of Q_a?, Nature, , 1976.

Marshall, P.D., D.L. Springer, H.C. Rodean, Magnitude corrections for attenuation in the upper mantle, Geophys. J. Roy. Astron. Soc., 1977.

McCowan, D.W., and R.T. Lacoss, Transfer functions for the seismic research observatory seismograph system, Bull. Seism. Soc. Am., 68, 501-512, 1978.

Murphy, J.R., and L.J. O'Brien, The correlation of peak ground acceleration amplitude with seismic intensity and other physical parameters, Bull. Seismol. Soc. Am., 67, 877-915, 1977.

North, R., Station magnitude bias - its determination, causes, and effects, Technical Note 1977-24, Lincoln Laboratory, M.I.T., April 1977.

North, R., Detection characteristics of the SRO stations in seismic discrimination, Semiannual Technical Summary, Lincoln Laboratory, September 1978.

Oliver, J., and B. Isacks, Deep earthquake zones, anomalous structures in the upper mantle, and the lithosphere, J. Geophys. Res., 72, 4259-4275, 1967.

Pho, H.T., and L. Behe, Extended distances and angles of incidence of P waves, Bull. Seism. Soc. Am., 62, 885-902, 1972.

Richter, C.F., Elementary Seismology, W.H. Freeman, and Co, San Francisco and London, 1958.

Ringdal, F., Maximum likelihood estimation of seismic event magnitude from network data, Technical Report No. 1, Vela Network Evaluation and Automatic Processing Research, Texas Instruments, March 1975.

Romanowicz, B.A., Seismic structure of the upper mantle beneath the United States by three-dimensional immersion of body wave arrival times, Submitted to Geophys. J. Roy. Astr. Soc., August, 1978.

Sengupta, M.K., The structure of the earth's mantle from body wave observations, Sc.D., Thesis, M.I.T., Cambridge, MA, 1975.

Sheppard, R.M., Jr., Values of LASA time station residuals, velocity and azimuth errors, Technical Note 1967-44, Lincoln Laboratory, M.I.T., September 1967.

Toksöz, M.N., M.K. Sengupta, The amplitude of P waves and magnitude corrections for deep focus earthquakes, J. Geophys. Res., 82, 20, 1977.

Trifunac, M.D. and B. Westermo, A note on the correlation of frequency-dependent duration of strong earthquake ground motion with the Modified Mercalli Intensity and the geologic conditions at the recording stations, Bull. Seismol. Soc. Am., 67, 917-927, 1977.

Vanek, J. et al., Procedure for determining station magnitude corrections within a selected system of reference stations, Izv. Earth Phys., no. 1, 1976.

ADDITIONAL REFERENCES

LePichon, X., J. Francheteau, J. Bonnin, Plate Tectonics, developments in geotectonics 6, Elsevier Scientific Publishing Company, New York 1973.

Lee, W.B. and S.C. Solomon, Inversion Schemes for Surface Wave Attenuation and Q in the Crust and the Mantle, Geophy. J.R. ast. Soc. 43, 1975.

Chinnery, M.A., Investigations of the Seismological Input to the Safety Design of Nuclear Power Reacters in New England, Annual Report, Lincoln Laboratory, M.I.T., August, 1978.

Molnar, P., and J. Oliver, Lateral Variations of Attenuation in the Upper Mantle and Discontinuities in the Lithosphere J. Geophys. Res. 74, 1969.

Solomon, S.C. and M.N. Toksöz, Lateral Variations of Attenuation of P and S Waves Beneath the United States, Bull. Seismol. Soc. Am. 60, 1970.

Romney, B.C., et al., Travel Times and Amplitudes of Principal Body Phases Recorded From Gnome, Bull. Seismol. Soc. Am., 52, 1962.

Evernden, J.F. and D.M. Clark, Study of Teleseismic P. II Amplitude Data, Phys. Earth. Planet. Inter. 4, 1970.

von Seggern, D., Joint Magnitude Determination and Analysis of Variance for Explosion Magnitude Estimates, Bull. Seism. Soc. Am., 63, 1973.

Bullen, K.E., An Introduction to the Theory of Seismology, Cambridge University Press, 1965.

Evernden, J.F., and D.M. Clark, Study of Teleseismic P II - Amplitude Data, Phys. Earth. Planet. Int., 4, 1969.

Chinnery, M.A., Scatter in observed m_b values, SATS, Seismic Discrimination, March 1979.

Evernden, J.F., and W.M. Kohler, Bias in estimates of m_b at small magnitudes, Bull. Seismol. Soc. Am., 66, No. 6, 1976.

Chinnery, M.A., Towards the Elimination of Bias in Body Wave Magnitude, Paper presented at the U.S.G.S. Conference on the Determination of Earthquake Parameters, Denver, Colorado, March 1979.

Aki, K., Scattering of P waves under the Montana LASA, J. Geophys. Res., 78, No. 8, 1973.

Johnston, J.C., and M.A. Chinnery, Measurement of m_b using SRO Data, SATS - Lincoln Laboratory, September 1978.

List of Tables

TABLE I: 28 STATION NETWORK

STATION CODE	LOCATION
ALQ	Albuquerque, N.M.
BHA	Broken Hill, Zambia
•BMO	Blue Mtns., Oregon
BNS	Bensberg, Germany
BUL	Bulawayo, Rhodesia
CAN	Canberra, Australia
CLK	Chileka, Malawi
COL	College, Alaska
COP	Copenhagen, Denmark
EUR	Eureka, Nevada
KEV	Kevo, Finland
KHC	Czechoslovakia
KJN	Kajaani, Finland
LJU	Ljubljana, Yugoslavia
MBC	Mould Bay, Canada
MOX	Moxa, Germany
NOR	Nord, Greenland
NP-	Northwest Territories, Canada
NUR	Nurmijarvi, Finland
PMG	Port Moresby, New Guinea
PRE	Pretoria, South Africa
PRU	Czechoslovakia
RES	Resolute, Canada
SJG	San Juan, Puerto Rico
•TFO	Tonto Forest, Arizona
TUC	Tucson, Arizona
•UBO	Uinta Basin, Utah
WIN	Windhoek, South Africa

Table II

Percent Saturation as a Function of log A/T for Various Typical Magnification Factors

% Saturation	Magnification					
	400K	200K	100K	50K	25K	12.5K
100	2.6	2.9	3.2	3.5	3.8	4.1
75	2.4	2.7	3.0	3.3	3.6	4.0
50	2.3	2.6	2.9	3.2	3.5	3.8
25	2.0	2.3	2.6	2.9	3.2	3.5
12.5	1.7	2.0	2.3	2.6	2.9	3.2
6.25	1.5	1.7	2.0	2.3	2.6	2.9

Table III

source / receiver	Region 1	2	3	4	5	6	7	8	9	10	11
Germany											
BNS				-0.09	+0.01	+0.02				-0.08	
CLL			-0.04	-0.01	+0.18	-0.04				-0.21	
FUR			+0.21	+0.04	-0.09	-0.15				+0.07	+0.01
GRF				+0.09	0.0					0.0	
MOX			+0.05	-0.04	+0.09	-0.03	+0.25			-0.07	
STU				+0.12	+0.03	-0.13					
East Africa											
BHA			+0.05	+0.10						+0.01	-0.16
CIR			+0.04						+0.15	-0.03	-0.02
CLK			-0.15						+0.07	-0.21	+0.23
KRR			-0.06						+0.10	+0.05	+0.08
Western U.S.											
DUG				-0.08	-0.07	-0.07			+0.18		
EUR	-0.10			-0.08	+0.05	-0.07	+0.07	-0.10	-0.01		
TFO				-0.09	-0.13	-0.06	0.0		+0.15		
TUC					-0.25	+0.02			+0.08		
UBO				-0.13	-0.03	+0.03	+0.05	-0.01	0.0		-0.09

Table IV

Name	Lat.	Long	Elevation	Burial	Location
ANMO	34 56 30.0 N	106 27 30.0 W	1750	100	Albuquerque, New Mexico, US
ANTO	39 55 00.0 N	32 49 00.0 E	APPROXIMATE		Ankara, Turkey
BCAO					Bangui, Central African Rep
BOCO	4 37 23.0 S	74 03 54.0 W	APPROXIMATE		Bogata, Columbia
CHTO	18 47 24.0 N	98 58 37.0 E	416	100	Chiang Mai, Thailand
GUMO	13 35 16.0 N	144 51 58.6 E	14	123	Guam, Marianas Islands
A KAAO	34 32 27.0 N	69 02 35.4 E	APPROXIMATE		Kabul, Afganistan
MAIO	36 18 00.0 N	59 29 40.2 E	1000	100	Mashad, Iran
NWAO	32 55 35.4 S	117 14 13.2 E	327	100	Narrogin, Western Australia
QUPO	30 11 18.0 N	66 57 00.0 E	APPROXIMATE		Quetta, Pakistan
SHIO	25 34 00.0 N	91 53 00.0 E	APPROXIMATE		Shillong, India
SNZO	41 18 37.0 S	174 42 16.7 E	-12	100	South Karori, New Zealand
TATO	24 58 33.6 N	121 29 19.8 E	5	100	Taipei, Taiwan
A CTAO	20 05 18.0 S	146 15 16.0 E	357	37	Charters Towers, Australia
A MAJO	36 32 30.0 N	138 12 32.0 E	APPROXIMATE		Matsushiro, Japan
A ZOBO	16 16 12.0 S	68 07 30.0 W	4450	300	Zongo Valley, Bolivia

List of Figures

Fig. 13. Histogram of listed (SDAC) m_b minus (A)SRO mean m_b (with $N \geq 3$ stations, $h \leq 100$ km, all regions).

Fig. 14. Two events from the Aleutians.

Fig. 15. Azimuthal map centered on Fox Islands. Stations plotted are MAIO, KAAO, CHTO, CTAO, and ALQ (counter-clockwise, from top).

Fig. 16. m_b from 9 events from the Aleutians.

Fig. 17. Four events from the Indian Ocean.

Fig. 18. An event from Kamchatka, a b c unfiltered, d e high pass filtered to remove noise. The listed m_b for this event is 5.2, the listed depth is 22 km.

Fig. 19. Event parameters. Region: Kuril Islands; date: 22 March 1978; origin time: 0:50:35; location: 43.84°N, 148.91°E; depth: 47 km, m_b = 6.1 (SDAC Weekly Event Summary).

Fig. 20. Synthetic Brune model waveform with P, pP, Δt = 4.0s.

Fig. 21. Synthetic Brune model waveform with P, pP, Δt = 1.0s.

Fig. 22. Synthetic Brune model waveform with P, pP, Δt = 0.5s.

Fig. 23. Event parameters. a) Region: Andreanoff Islands, date: 4 November 1977; origin time: 9:53:4; location 51.71°N, 176.05°W; depth: 95 km, m_b = 5.7. b) Region: Fox Islands; date: 23 November, 1977; origin time: 16:55:22; location: 51.94°N, 171.43°W; depth: 57 km, m_b = 5.5 (SDAC weekly event summary).

Fig. 24. Six events from the Kuril Islands. Depths range from 1 km to 54 km, listed m_b's range from 5.8 to 6.2.

Fig. 25. From Khalturin, Rautian and Molnar (19): events used that showed high frequencies and large amplitudes at recording stations in Garm, Faizabad, and Khorog.

Fig. 26. a) A Mid-Indian Rise event with a listed m_b of 4.7, depth listed as 0 km, delta for KAAO is 43.8° yielding an $m_b \sim 4.9$, delta for MAIO is 46.1 yielding an m_b of 4.5. b) An event from the Southeast-Indian Rise, listed $m_b = 4.7$, depth = 0 km, delta for KAAO = 41.0° yielding $m_b = 4.2$, delta for MAIO = 46.8° yielding an $m_b = 4.3$.

Fig. 27. Two events from Crete. a) listed depth = 2 km, listed $m_b = 4.6$ Δ(KAAO) = 35.8°, Δ(MAIO) = 27.8°. b) listed depth = 0 km, listed $m_b = 4.5$ Δ(KAAO) = 35.5°, Δ(MAIO) = 27.5°.

Figure 1

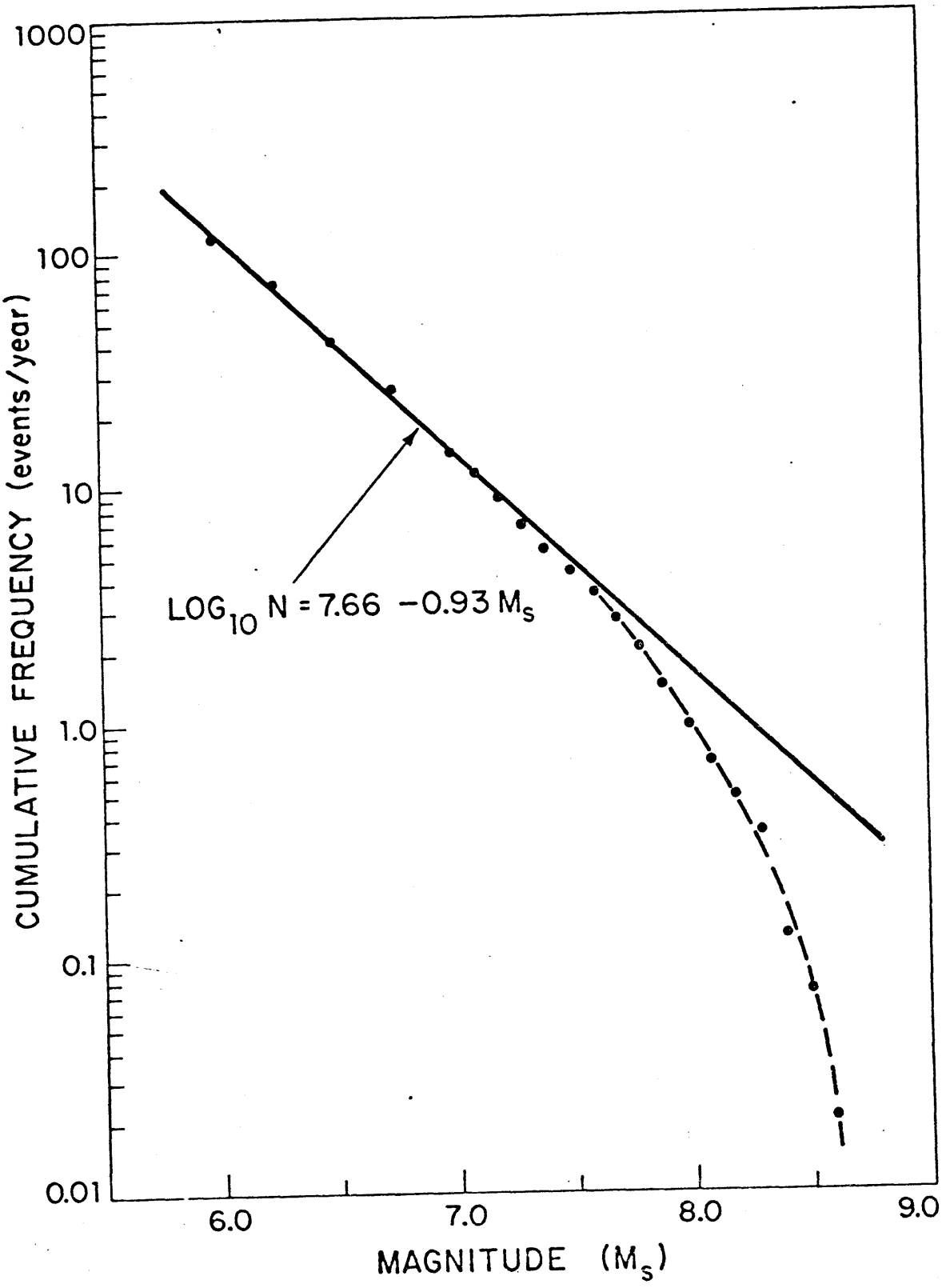
1000
100
10
1.0
0.1
0.01
CUMULATIVE FREQUENCY (events/year)
LOG10 N = 7.66 −0.93 Ms
6.0
7.0
8.0
9.0
MAGNITUDE (Ms)

Figure 2

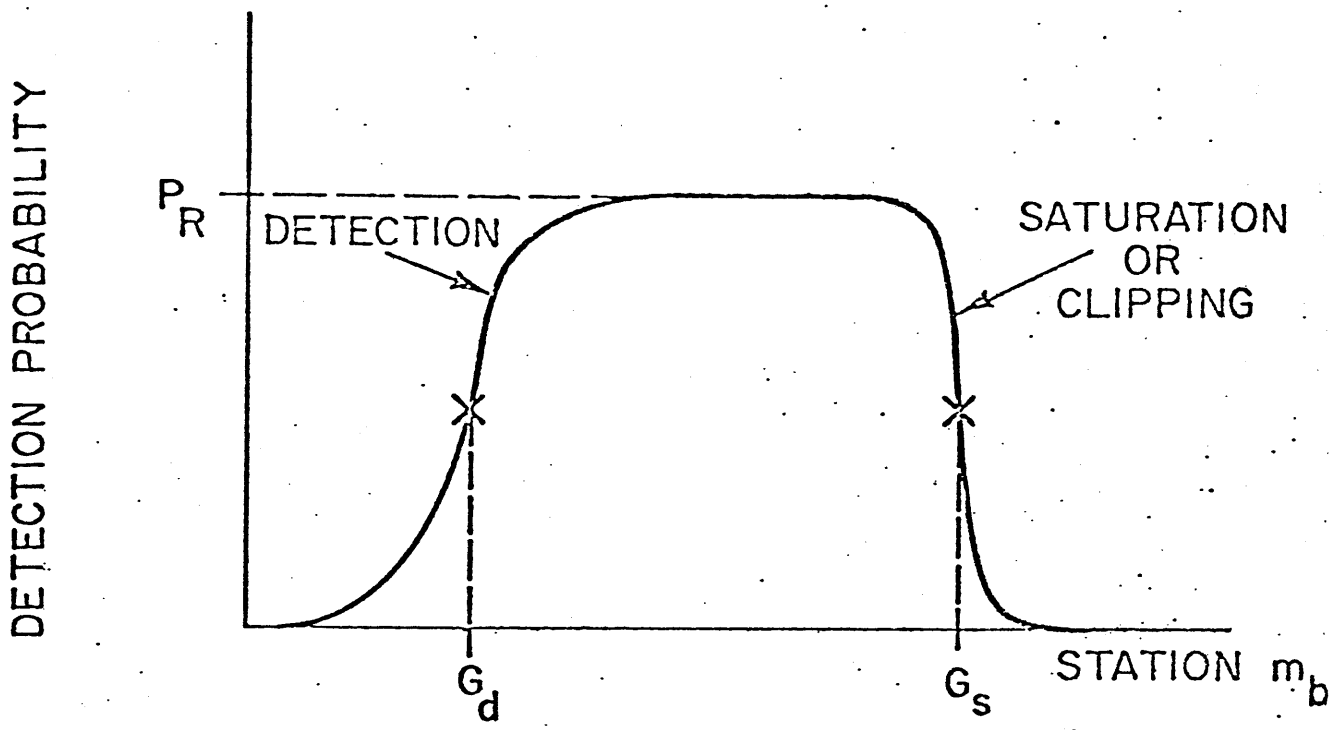

STATION DETECTION PARAMETERS

G_d	50% DETECTION THRESHOLD
γ_d	SPREAD OF DETECTION CURVE
G_s	50% SATURATION THRESHOLD
γ_s	SPREAD OF SATURATION CURVE
B	STATION MAGNITUDE BIAS
P_R	PROBABILITY OF REPORTING

Figure 3*

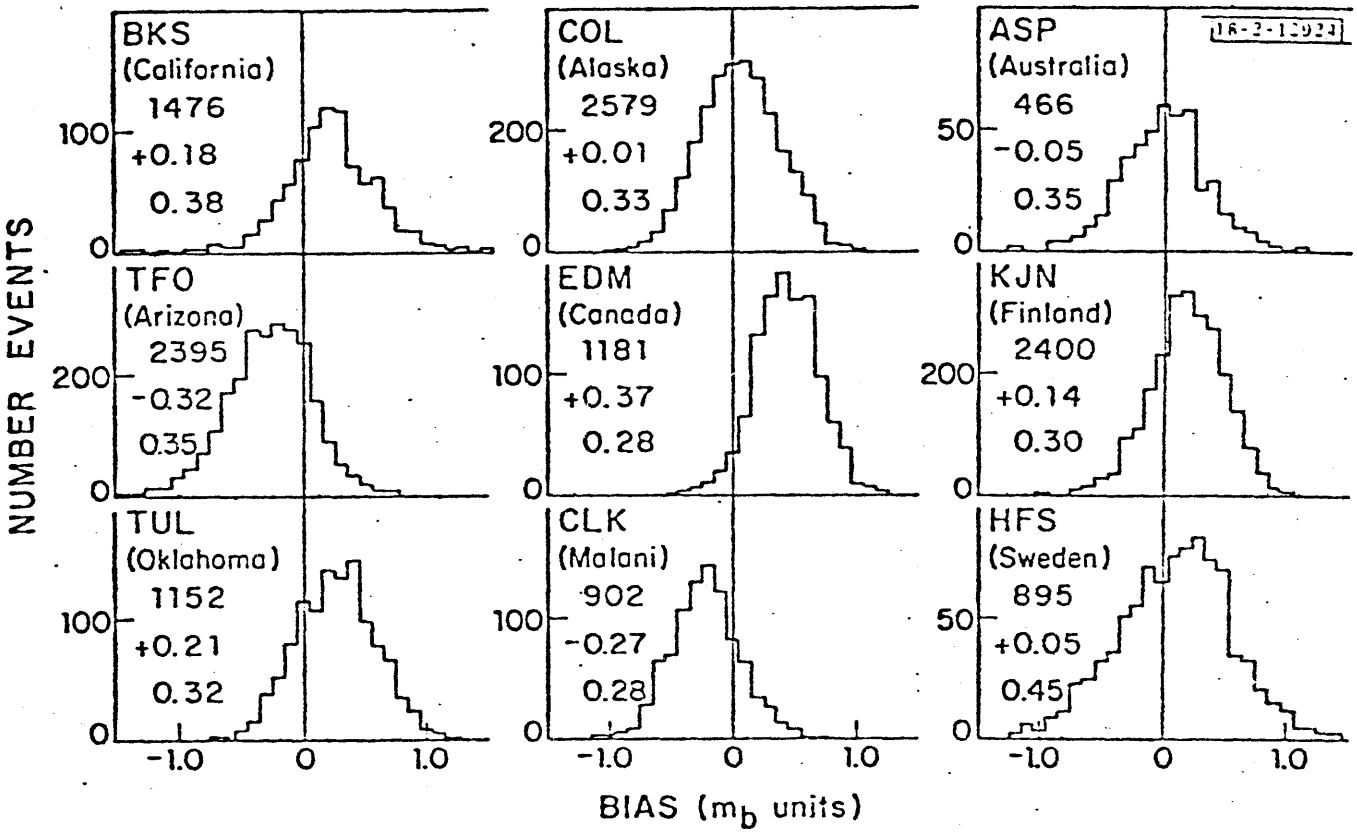

*from North 1977

Information Given:

station, location, number of events, average, and standard deviation

Figure 4*

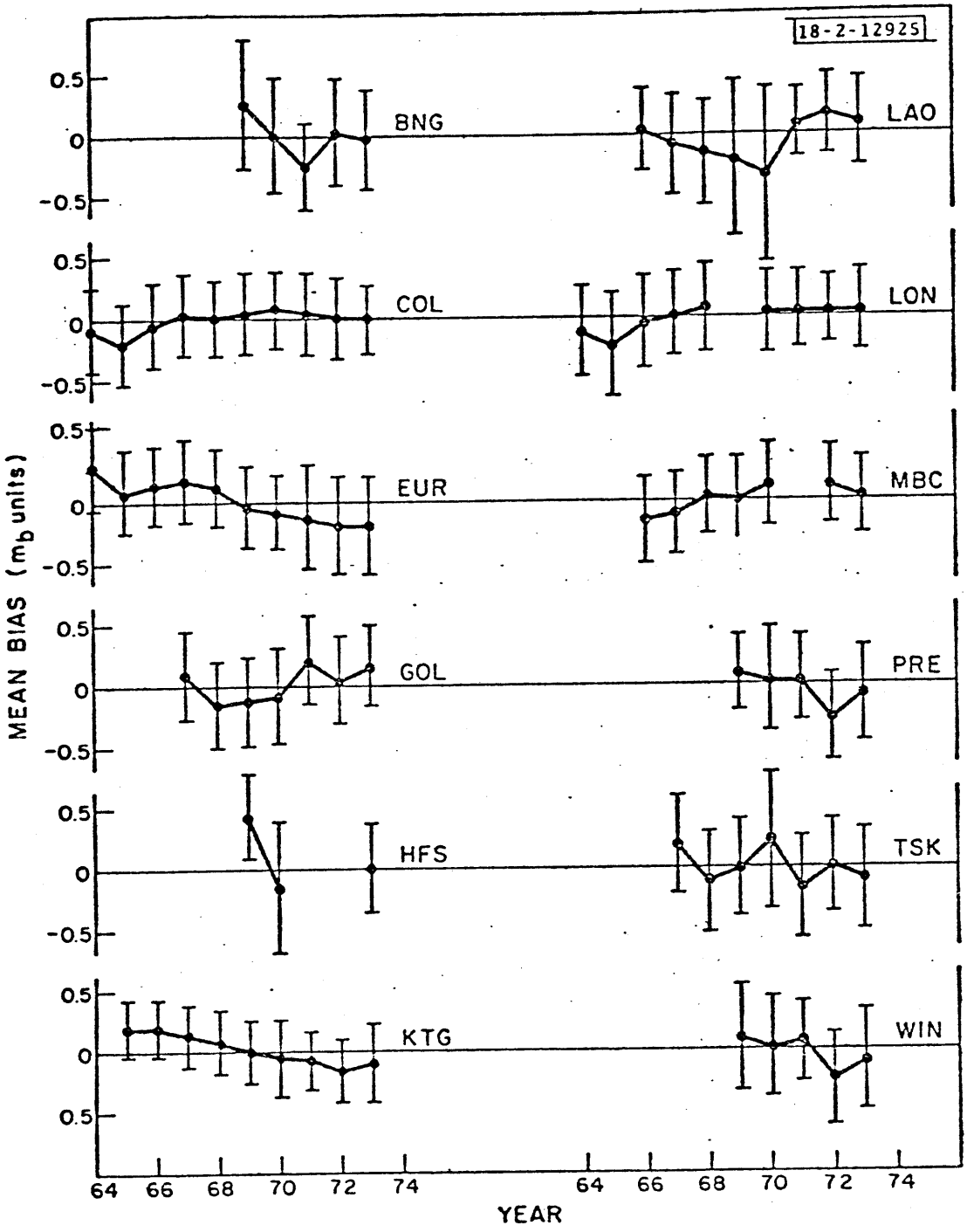

*from North 1977

Figure 5

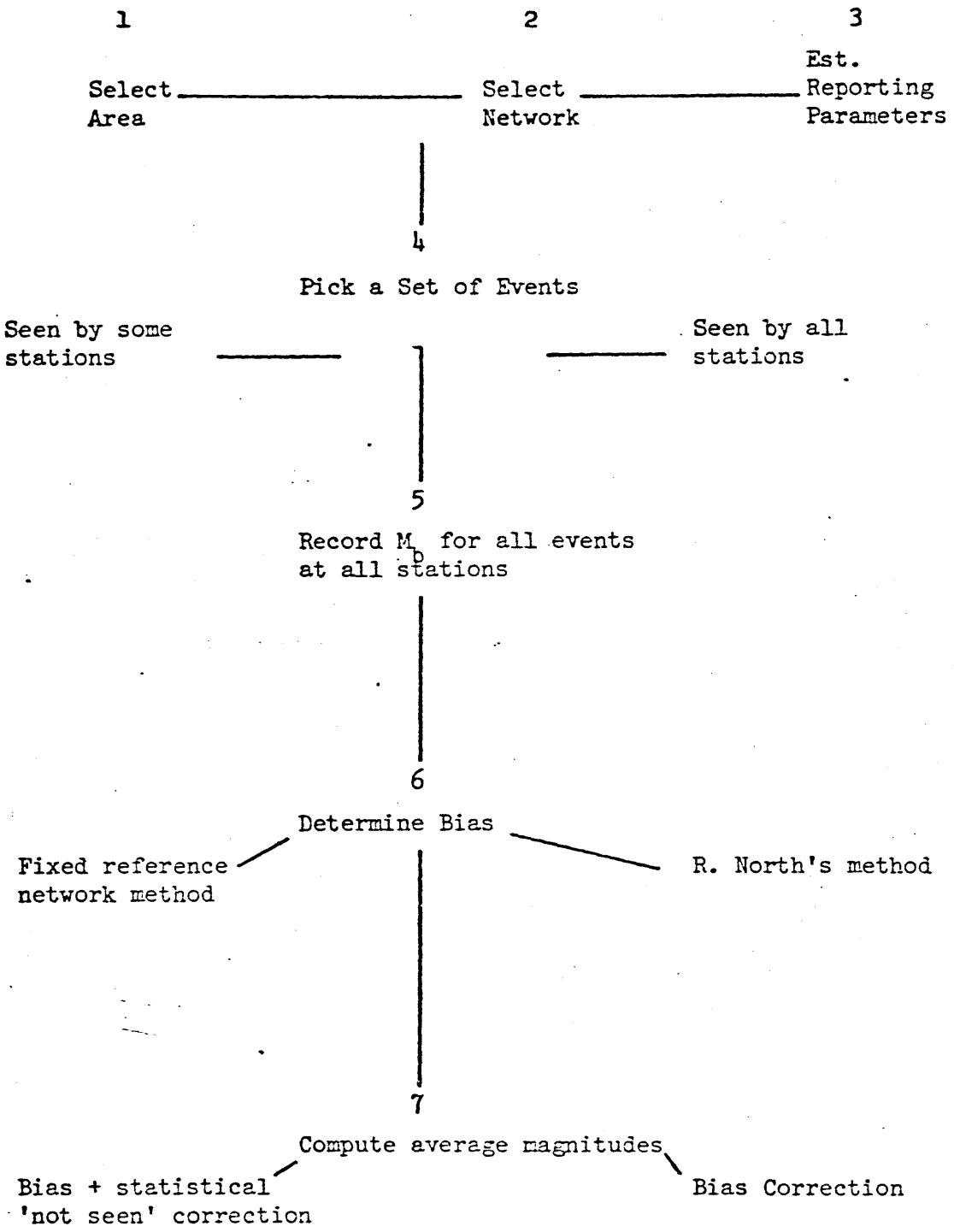
1
2
3
Select Area
Select Network
Est. Reporting Parameters
4
Pick a Set of Events
Seen by some stations
Seen by all stations
5
Record M_b for all events at all stations
6
Determine Bias
Fixed reference network method
R. North's method
7
Compute average magnitudes
Bias + statistical 'not seen' correction
Bias Correction

Figure 6

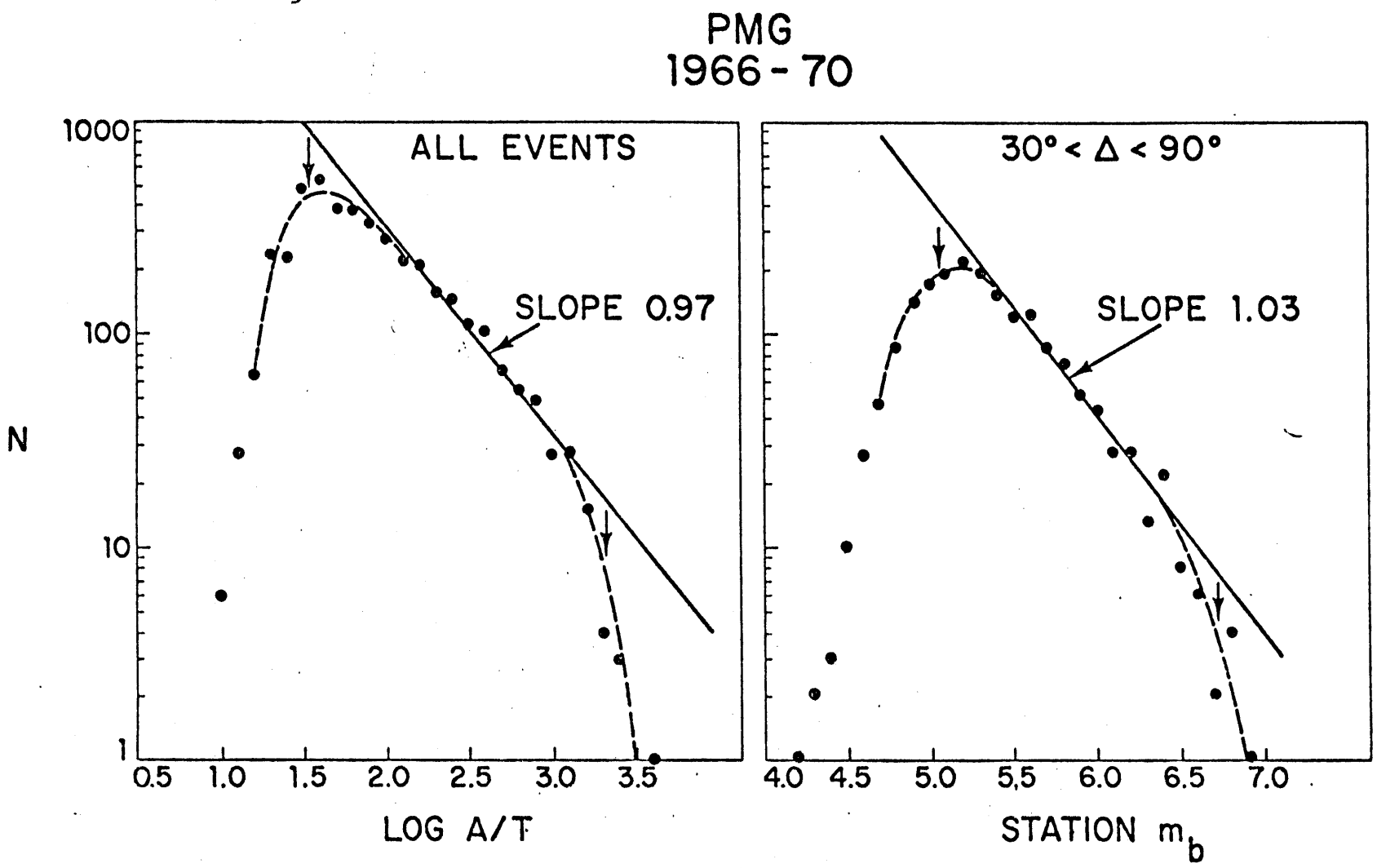
PMG
1966 - 70
ALL EVENTS
SLOPE 0.97
30° < Δ < 90°
SLOPE 1.03
N
1000
100
10
1
0.5
1.0
1.5
2.0
2.5
3.0
3.5
LOG A/T
4.0
4.5
5.0
5.5
6.0
6.5
7.0
STATION m_b

Figure 7

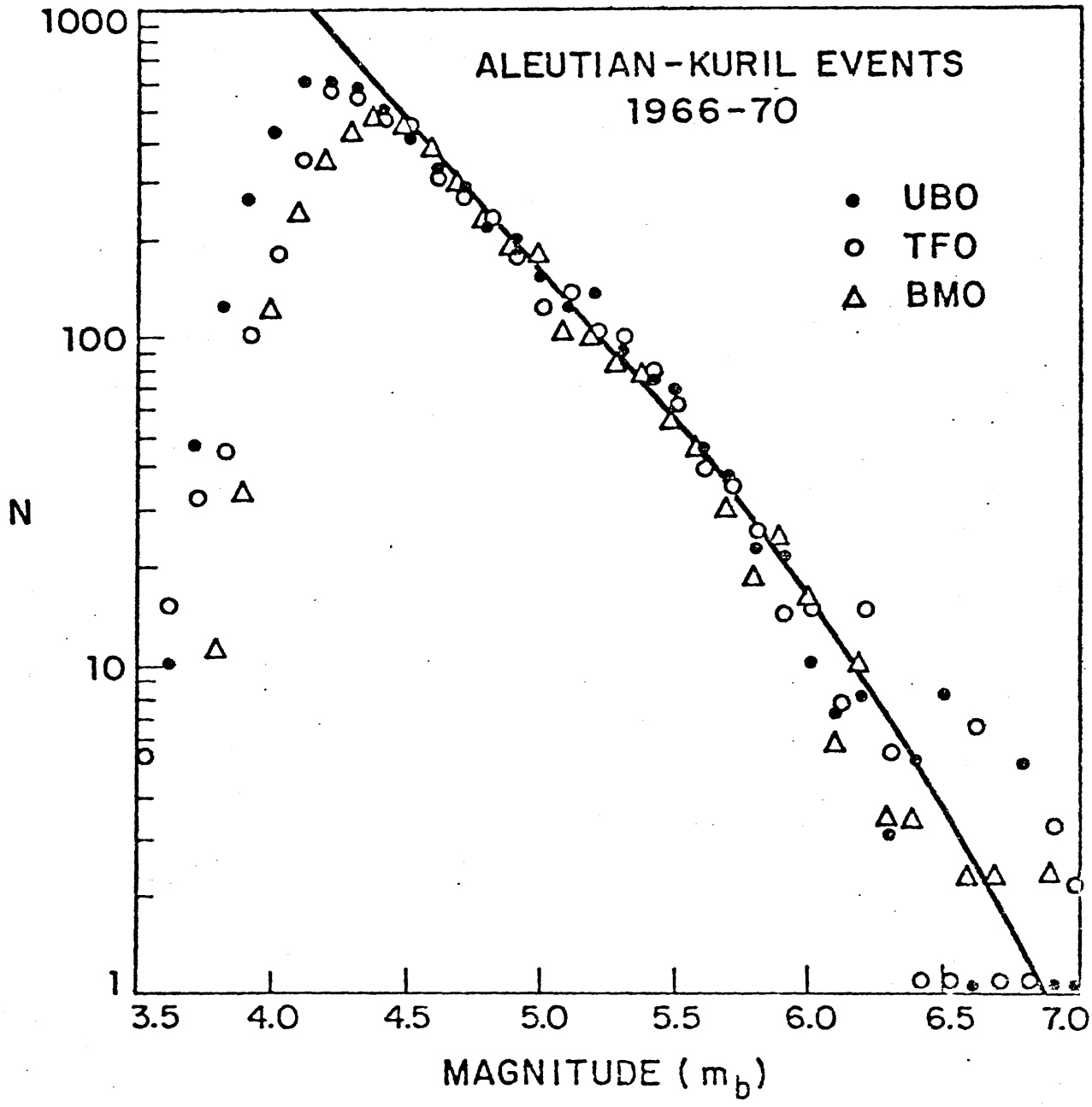
ALEUTIAN-KURIL EVENTS
1966-70
UBO
TFO
BMO
1000
100
10
1
N
3.5
4.0
4.5
5.0
5.5
6.0
6.5
7.0
MAGNITUDE (m_b)

Figure 8

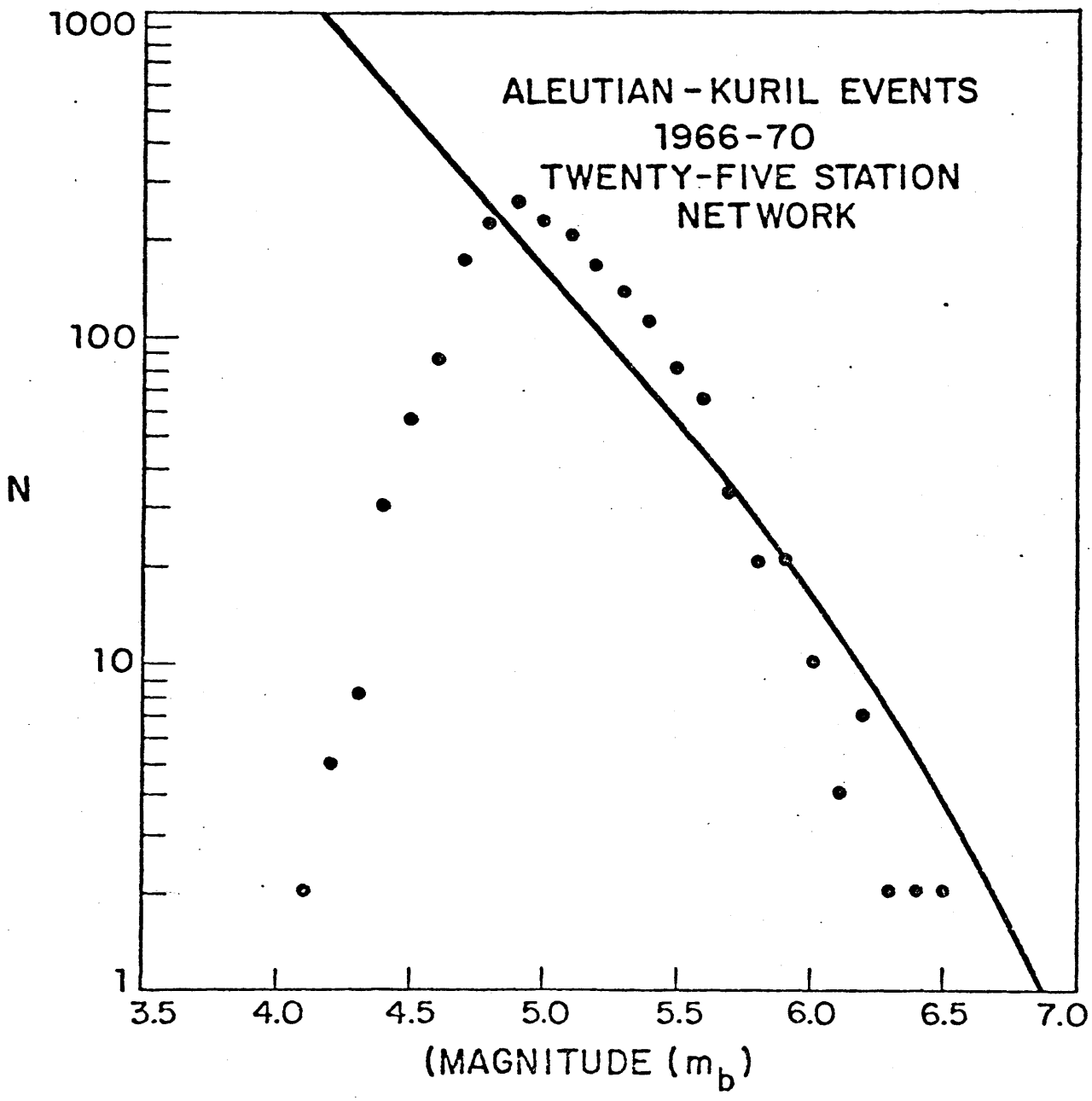
ALEUTIAN - KURIL EVENTS
1966-70
TWENTY-FIVE STATION
NETWORK
1000
100
10
1
N
3.5
4.0
4.5
5.0
5.5
6.0
6.5
7.0
(MAGNITUDE (m_b))

Figure 9

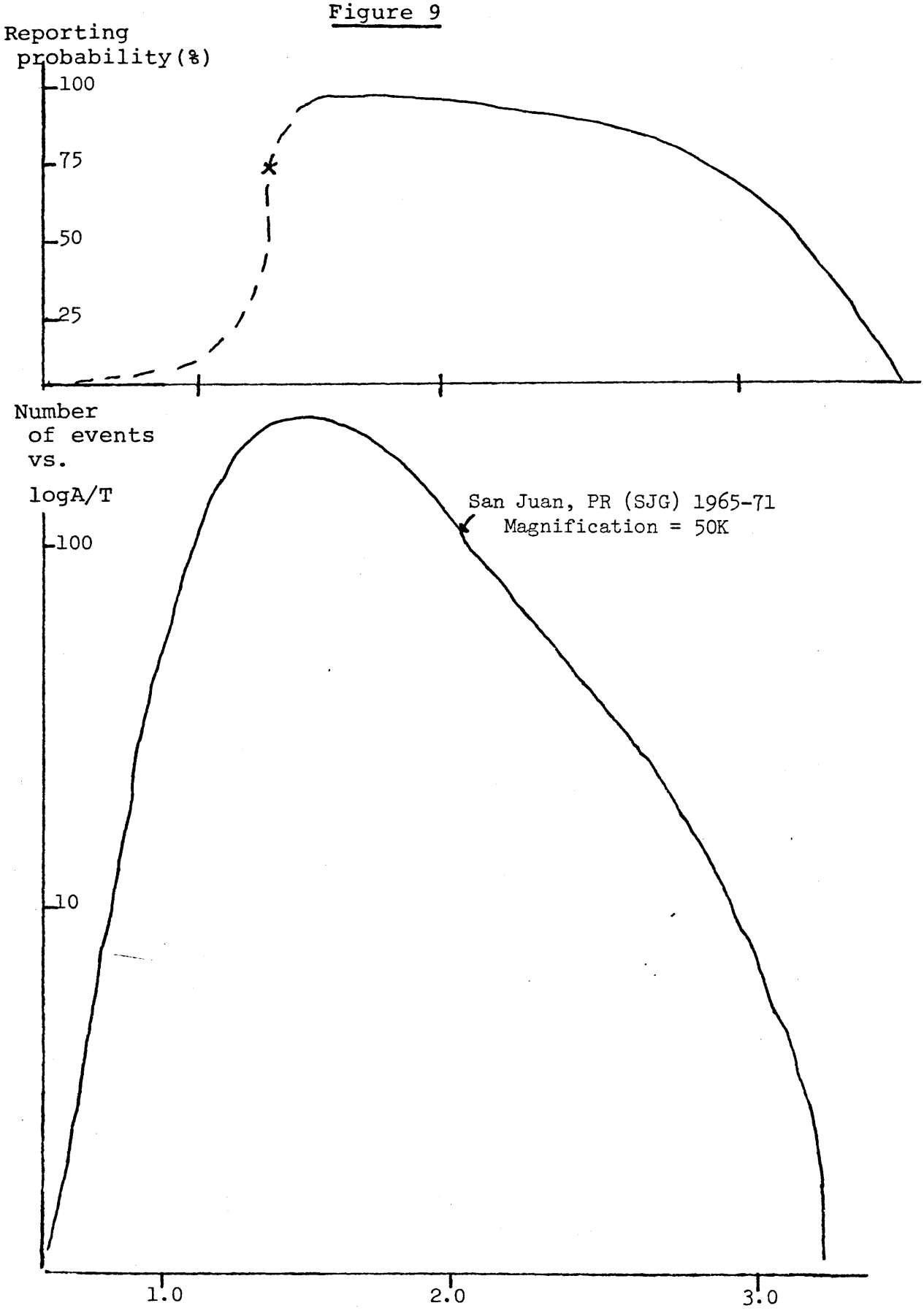
Reporting probability (%)
100
75
50
25
Number of events vs. logA/T
San Juan, PR (SJG) 1965-71
Magnification = 50K
100
10
1.0
2.0
3.0

Figure 10

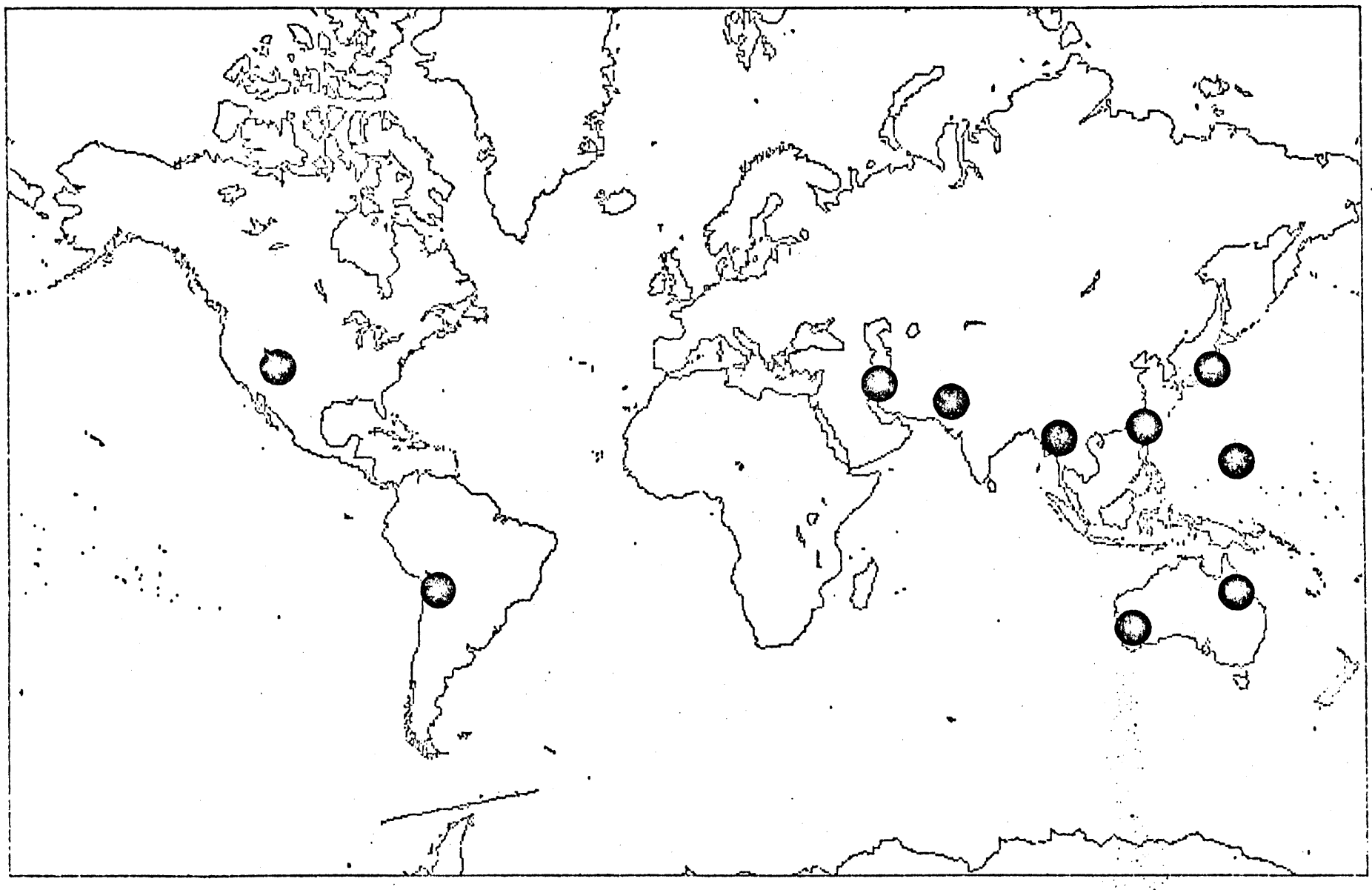

FIGURE 11

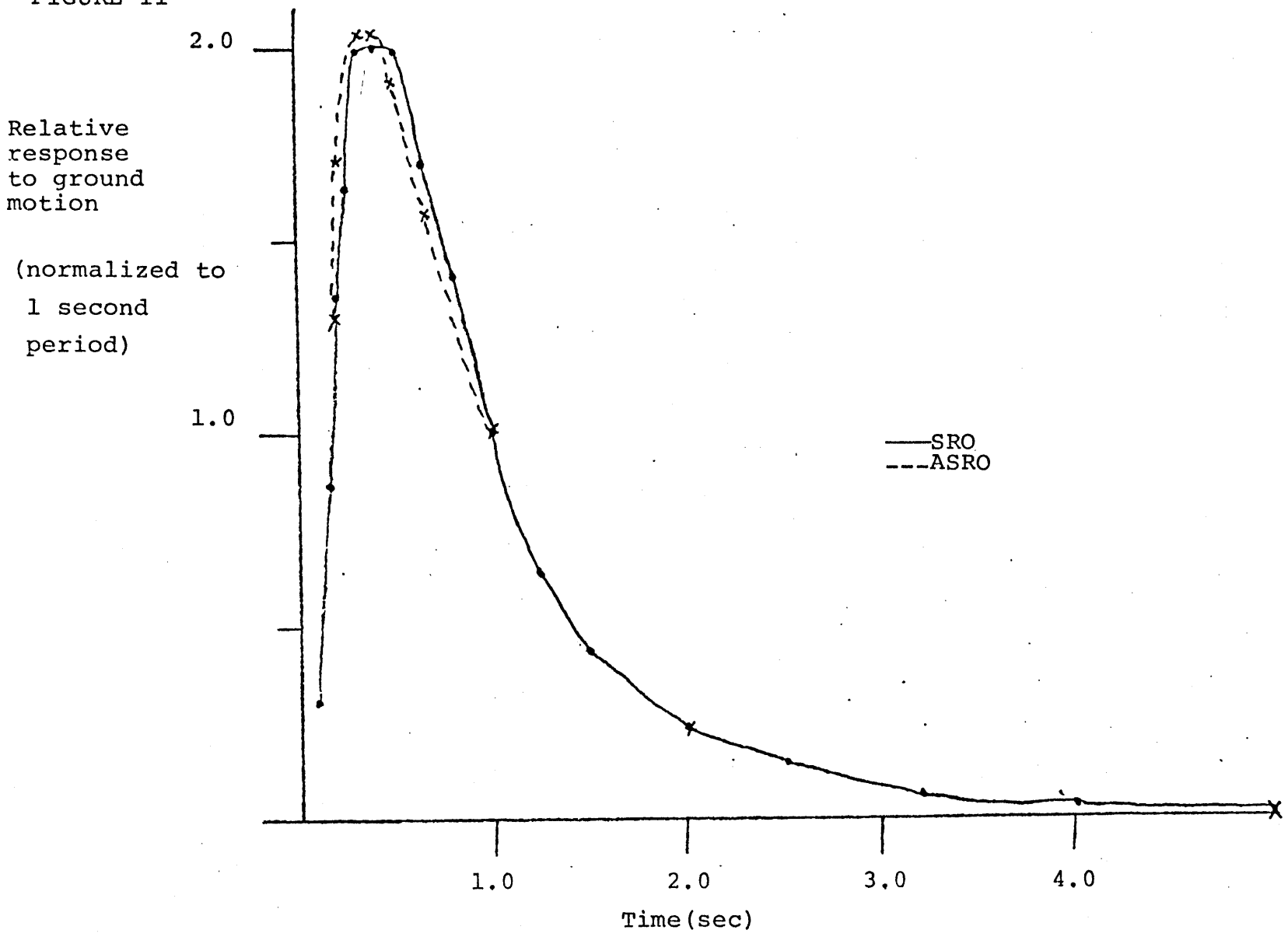
2.0
1.0
Relative response to ground motion
(normalized to 1 second period)
SRO
ASRO
1.0
2.0
3.0
4.0
Time(sec)

FIGURE 12

a)

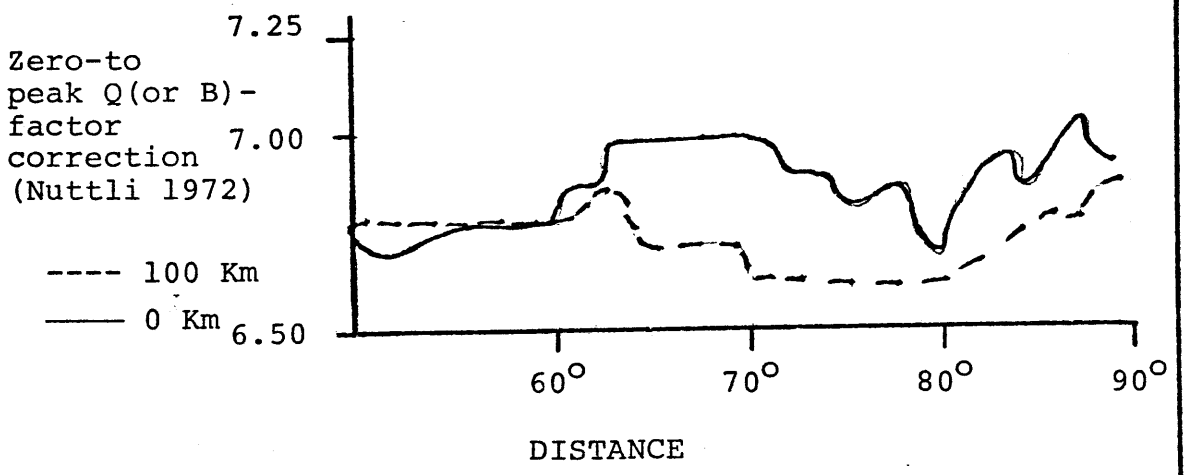

b)*

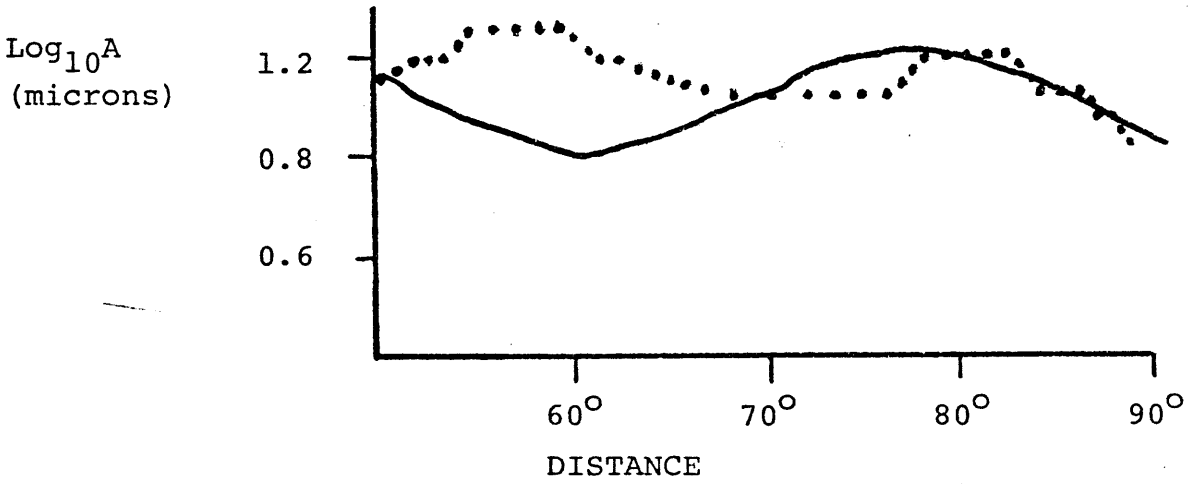

.... G&R(1958)
____Sengupta&Toksöz(1977)

*From Sengupta and Toksöz(1977)

Figure 13

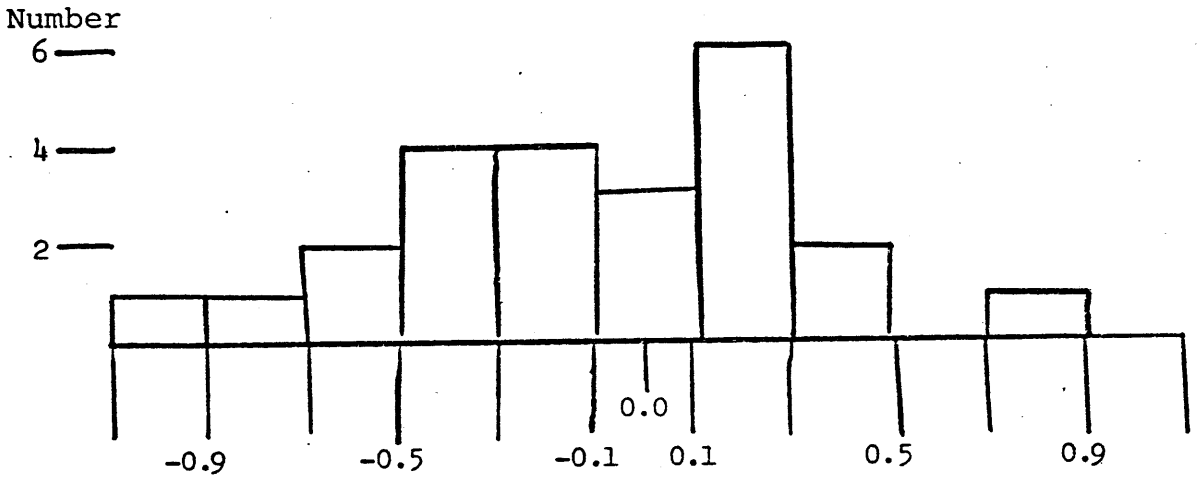

SDAC listed m_b minus mean (A)SRO m_b

Figure 14

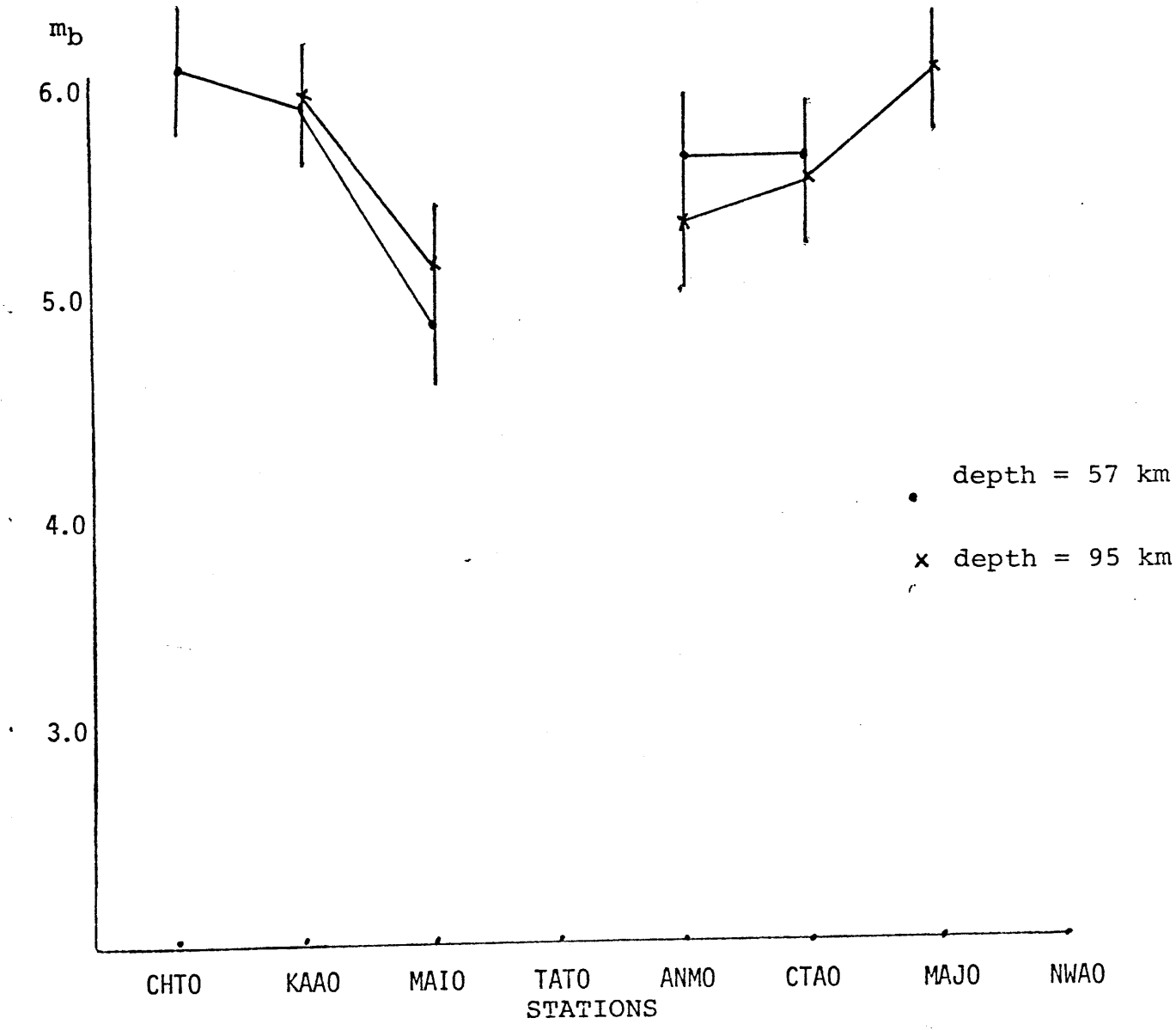
m_b
6.0
5.0
4.0
3.0
depth = 57 km
depth = 95 km
CHTO
KAAO
MAIO
TATO
ANMO
CTAO
MAJO
NWAO
STATIONS

Figure 15

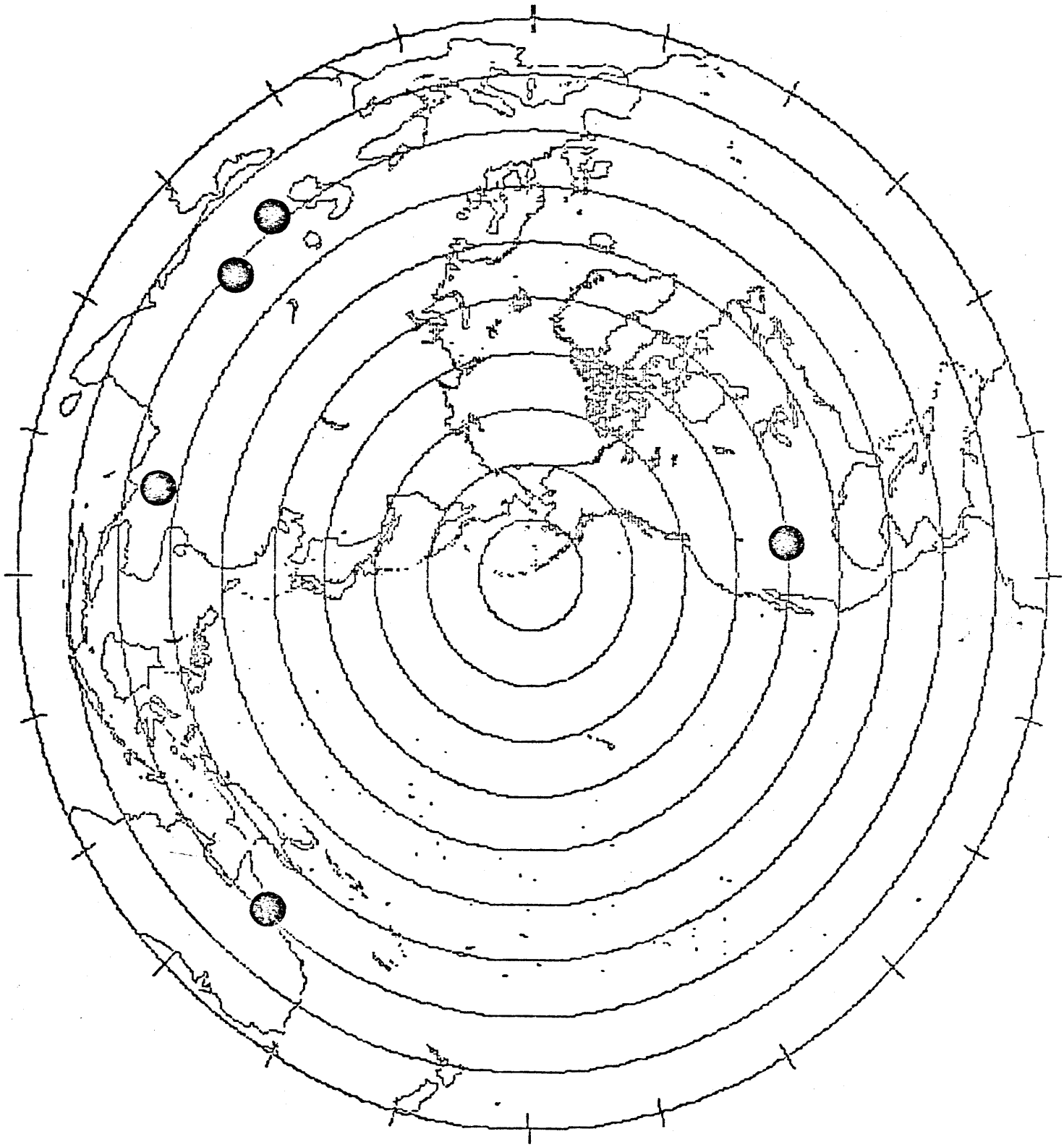

Figure 16

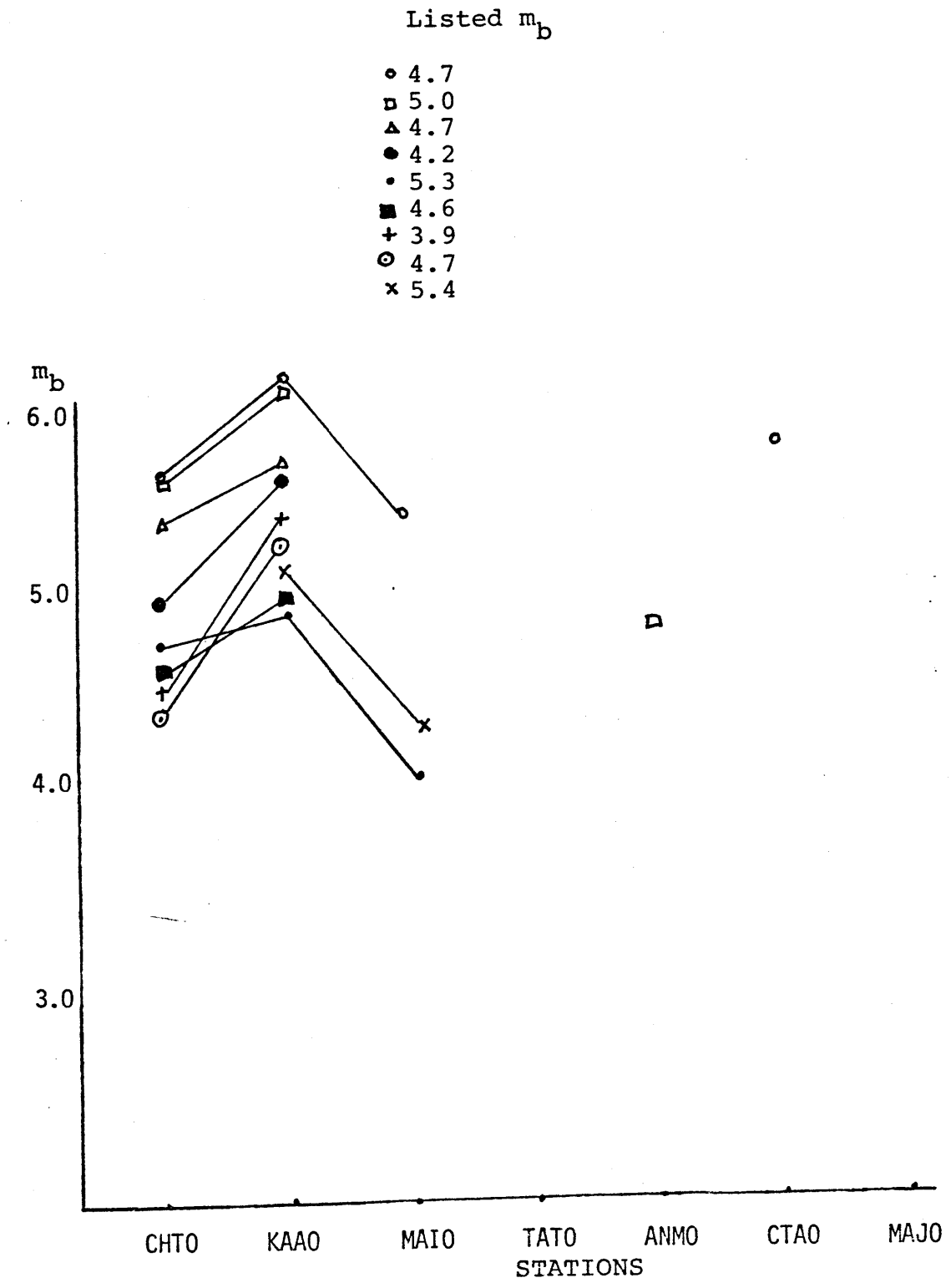
Listed m_b
4.7
5.0
4.7
4.2
5.3
4.6
3.9
4.7
5.4
m_b
6.0
5.0
4.0
3.0
CHTO
KAAO
MAIO
TATO
ANMO
CTAO
MAJO
STATIONS

Figure 17

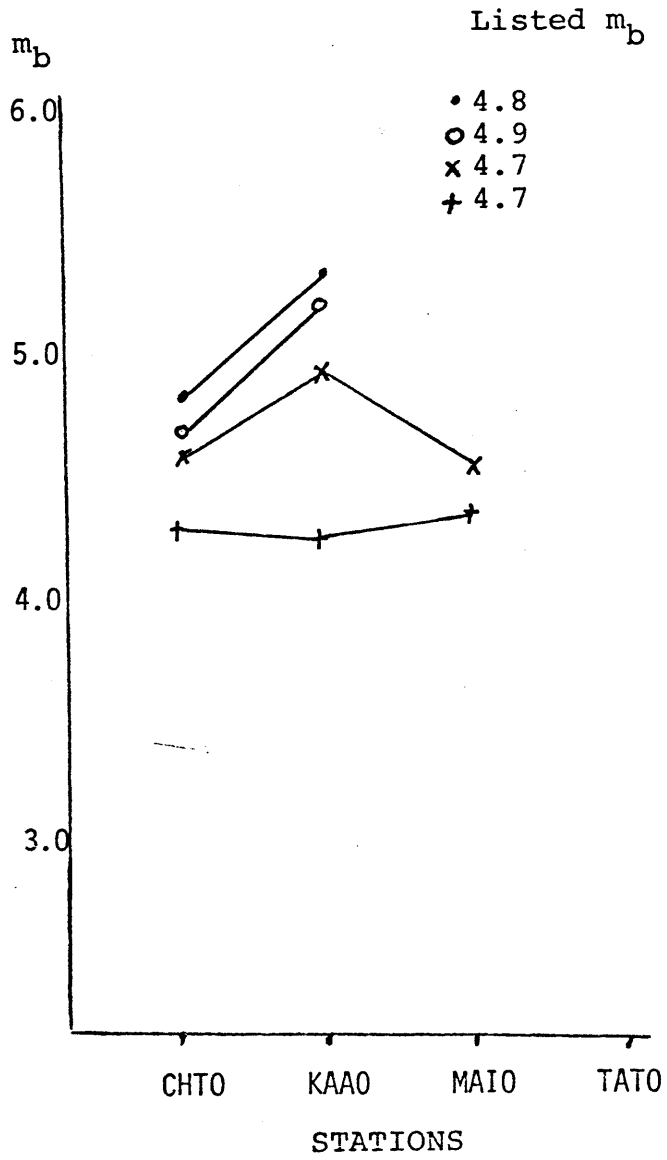
Listed m_b
m_b
6.0
5.0
4.0
3.0
• 4.8
o 4.9
× 4.7
+ 4.7
CHTO
KAAO
MAIO
TATO
STATIONS

Figure 18

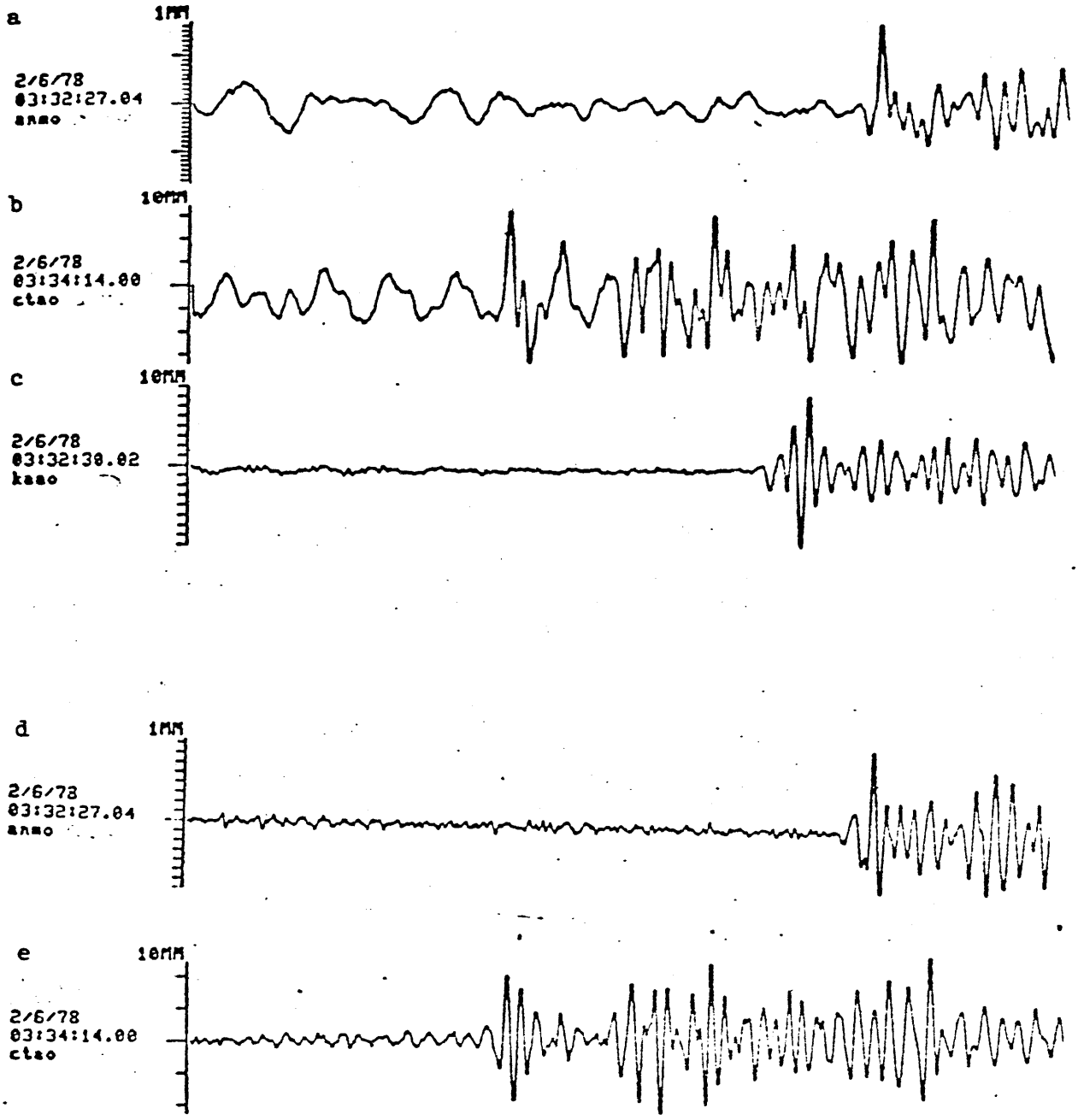
a
1MM
2/6/78
03:32:27.04
anmo
b
10MM
2/6/78
03:34:14.00
ctao
c
10MM
2/6/78
03:32:30.02
kaao
d
1MM
2/6/78
03:32:27.04
anmo
e
10MM
2/6/78
03:34:14.00
ctao

Figure 19

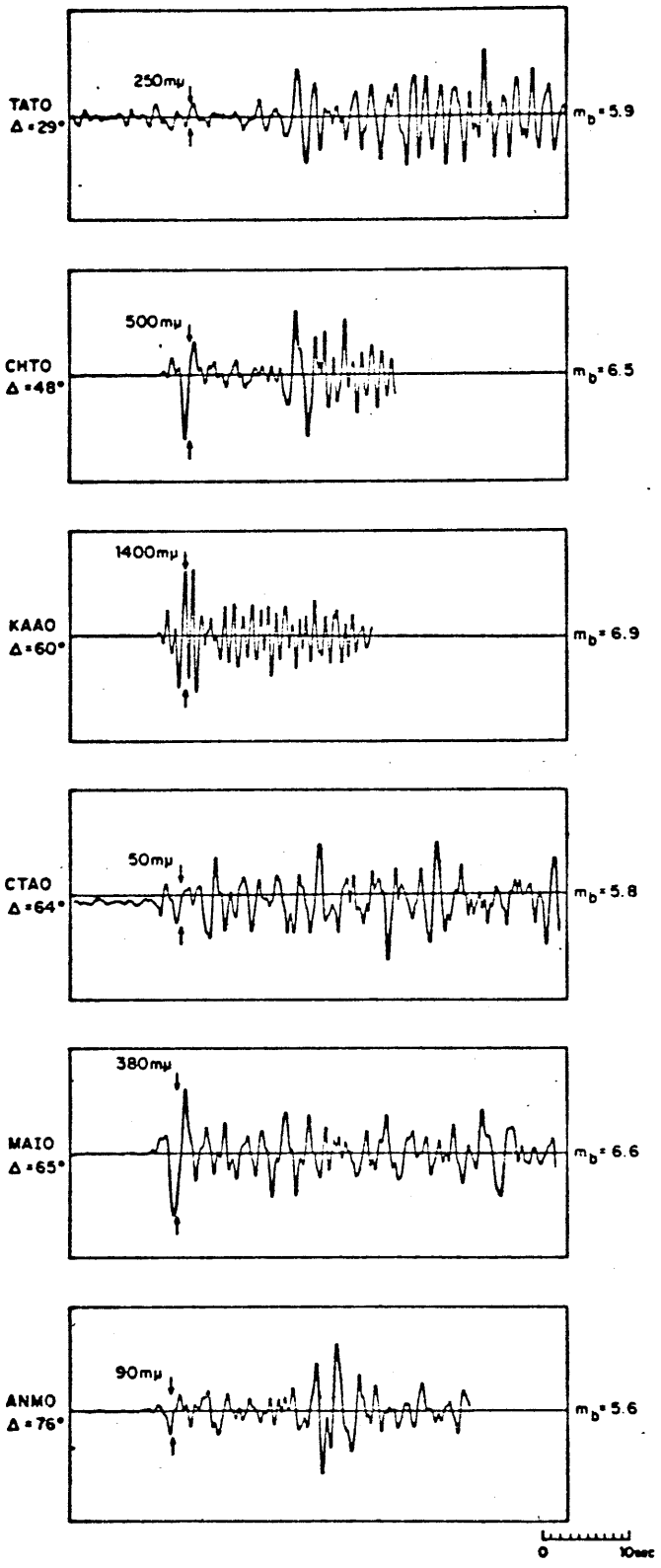
250mμ
TATO
Δ=29°
m_b=5.9
500mμ
CHTO
Δ=48°
m_b=6.5
1400mμ
KAAO
Δ=60°
m_b=6.9
50mμ
CTAO
Δ=64°
m_b=5.8
380mμ
MAIO
Δ=65°
m_b=6.6
90mμ
ANMO
Δ=76°
m_b=5.6
0
10sec

Figure 20

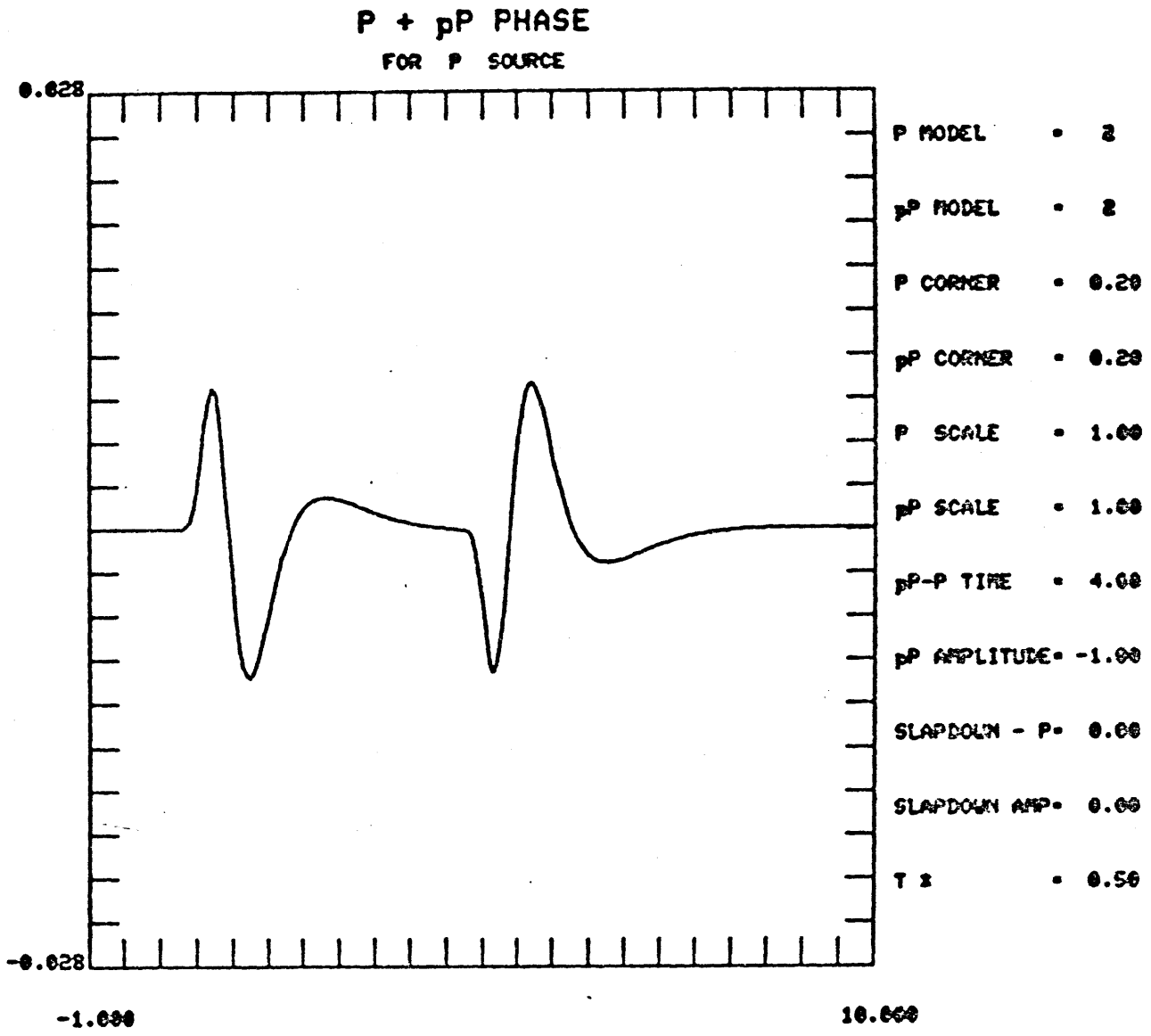
P + pP PHASE
FOR P SOURCE
0.028
-0.028
-1.000
10.000
P MODEL • 2
pP MODEL • 2
P CORNER • 0.20
pP CORNER • 0.20
P SCALE • 1.00
pP SCALE • 1.00
pP-P TIME • 4.00
pP AMPLITUDE • -1.00
SLAPDOWN - P • 0.00
SLAPDOWN AMP • 0.00
T 2 • 0.50

Figure 21

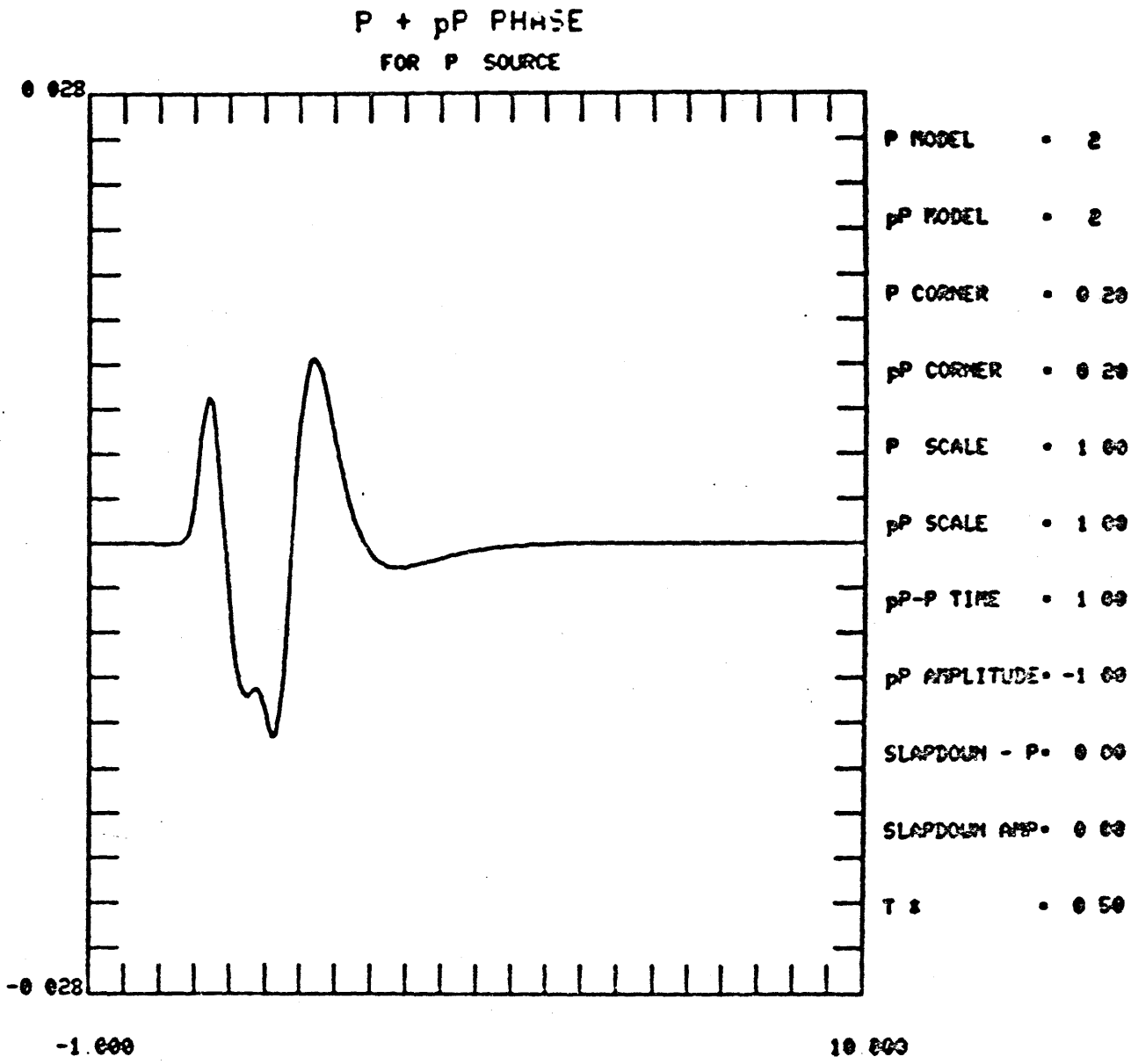
P + pP PHASE
FOR P SOURCE
0 028
-0 028
-1 000
10 000
P MODEL • 2
pP MODEL • 2
P CORNER • 0 20
pP CORNER • 0 20
P SCALE • 1 00
pP SCALE • 1 00
pP-P TIME • 1 00
pP AMPLITUDE • -1 00
SLAPDOWN - P • 0 00
SLAPDOWN AMP • 0 00
T ± • 0 50

Figure 22

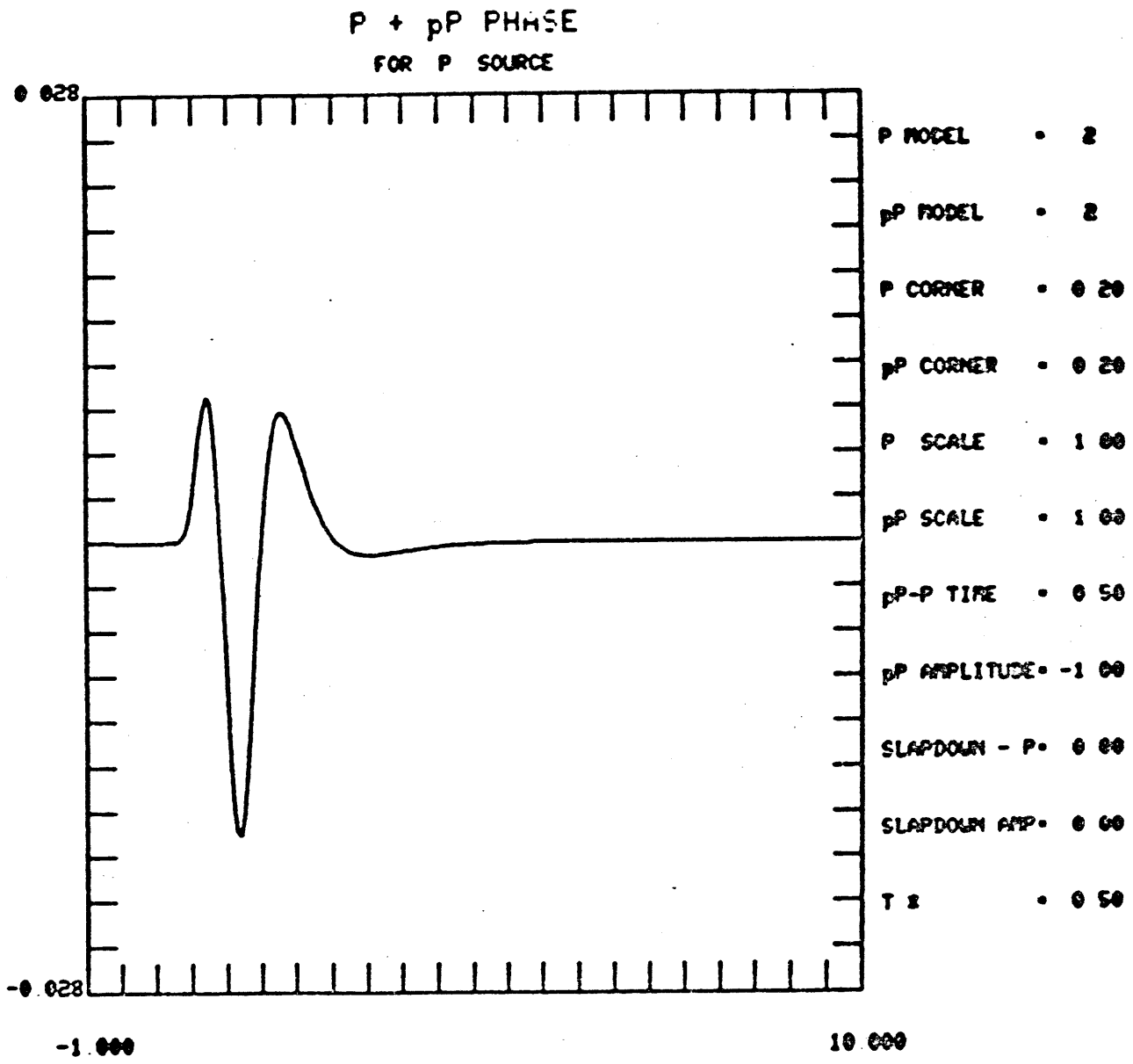
P + pP PHASE
FOR P SOURCE
0.028
-0.028
-1.000
10.000
P MODEL • 2
pP MODEL • 2
P CORNER • 0.20
pP CORNER • 0.20
P SCALE • 1.00
pP SCALE • 1.00
pP-P TIME • 0.50
pP AMPLITUDE • -1.00
SLAPDOWN - P • 0.00
SLAPDOWN AMP • 0.00
T 2 • 0.50

Figure 23 a

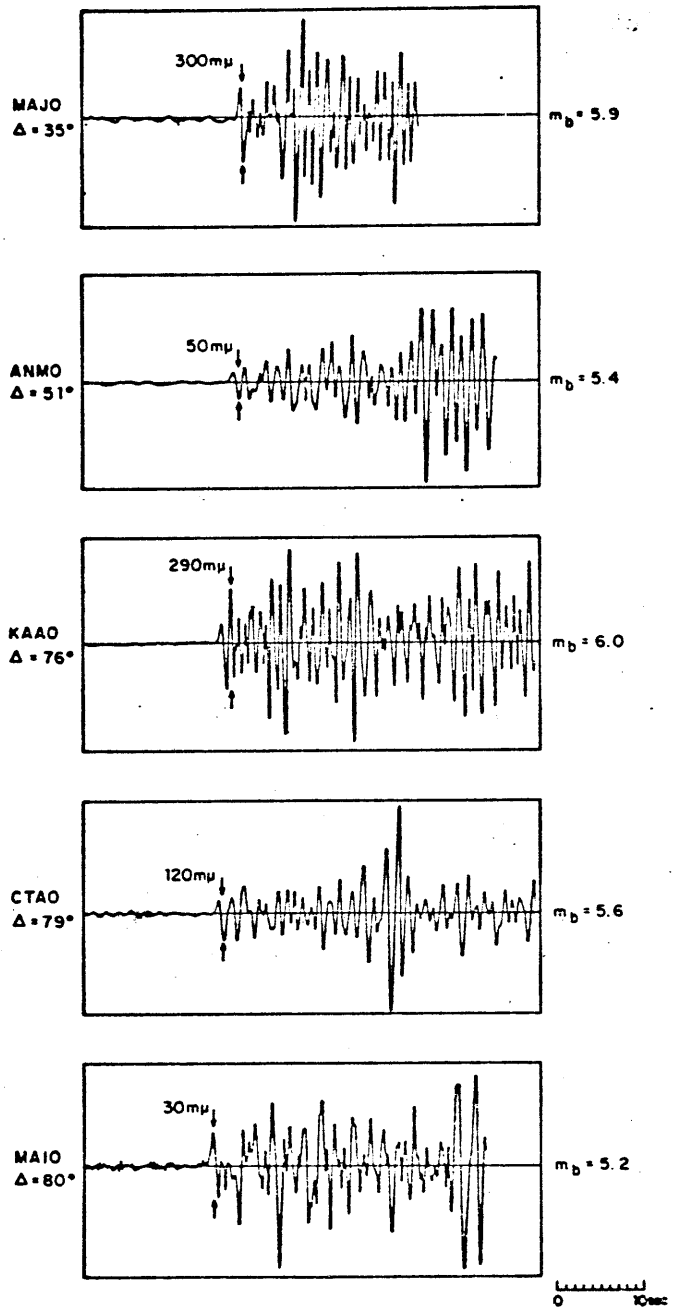
300mμ
MAJO
Δ = 35°
m_b = 5.9
50mμ
ANMO
Δ = 51°
m_b = 5.4
290mμ
KAAO
Δ = 76°
m_b = 6.0
120mμ
CTAO
Δ = 79°
m_b = 5.6
30mμ
MAIO
Δ = 80°
m_b = 5.2
0
10sec

Figure 23 b.

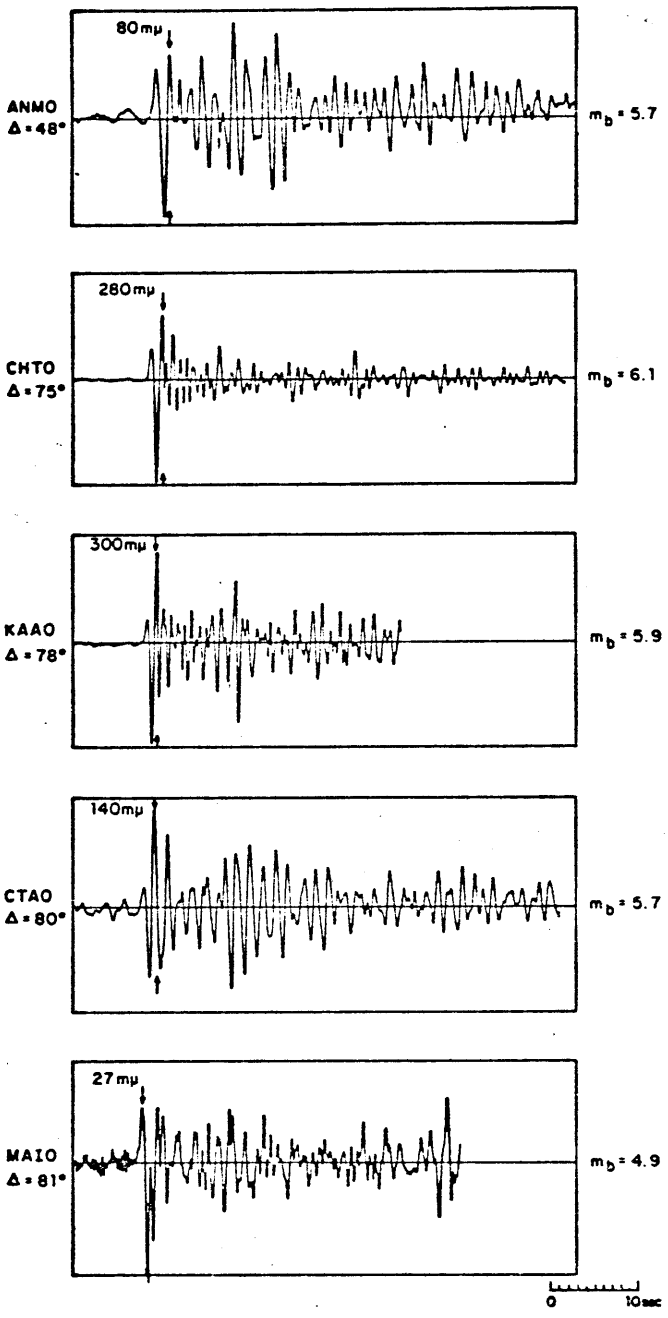
80mμ
ANMO
Δ = 48°
m_b = 5.7
280mμ
CHTO
Δ = 75°
m_b = 6.1
300mμ
KAAO
Δ = 78°
m_b = 5.9
140mμ
CTAO
Δ = 80°
m_b = 5.7
27mμ
MAIO
Δ = 81°
m_b = 4.9
0
10sec

Figure 24

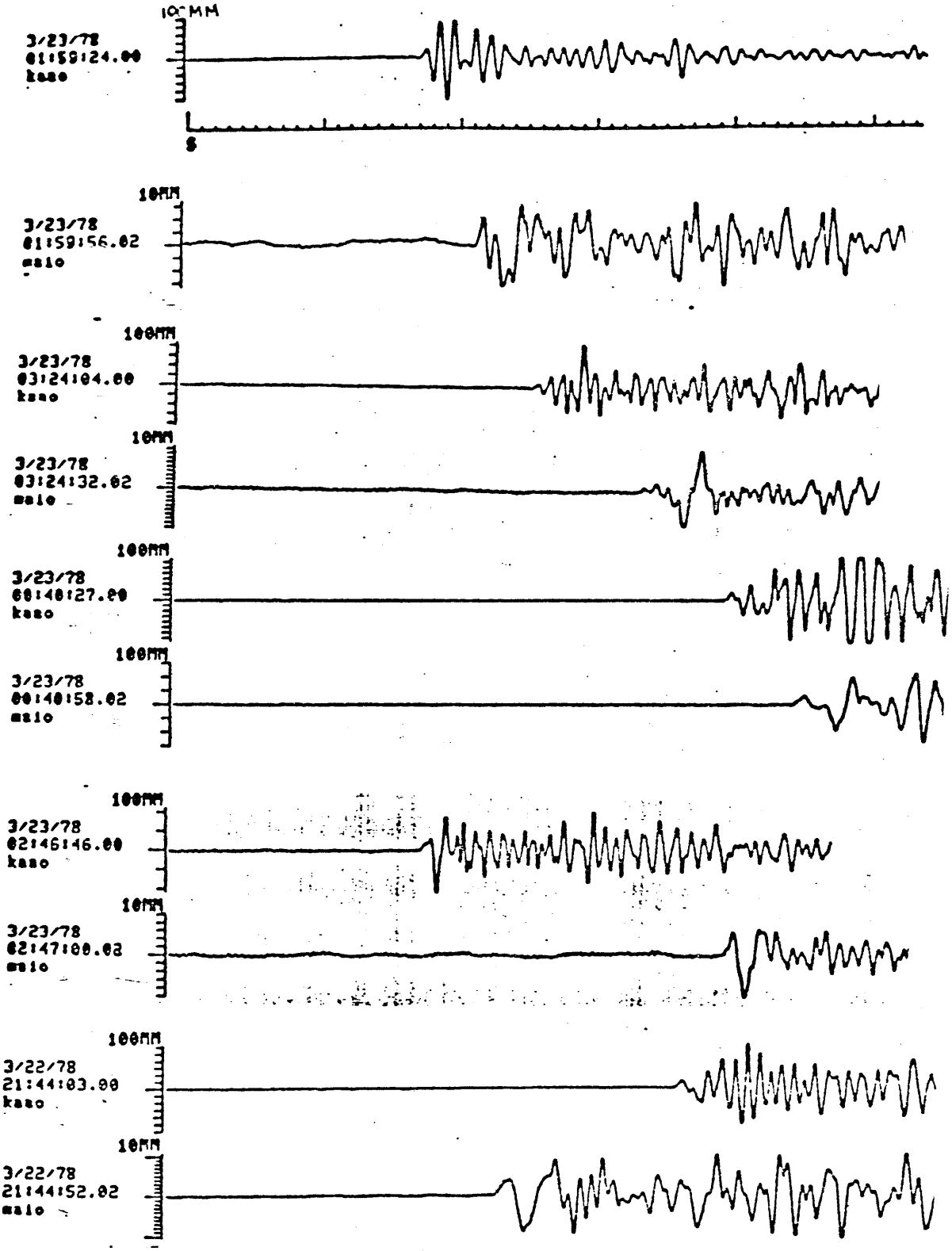
10 MM
3/23/78
01:59:24.00
kaso
S
10MM
3/23/78
01:59:56.02
mslo
100MM
3/23/78
03:24:04.00
kaso
10MM
3/23/78
03:24:32.02
mslo
100MM
3/23/78
00:40:27.00
kaso
100MM
3/23/78
00:40:58.02
mslo
100MM
3/23/78
02:46:46.00
kaso
10MM
3/23/78
02:47:00.02
mslo
100MM
3/22/78
21:44:03.00
kaso
10MM
3/22/78
21:44:52.02
mslo

Figure 25

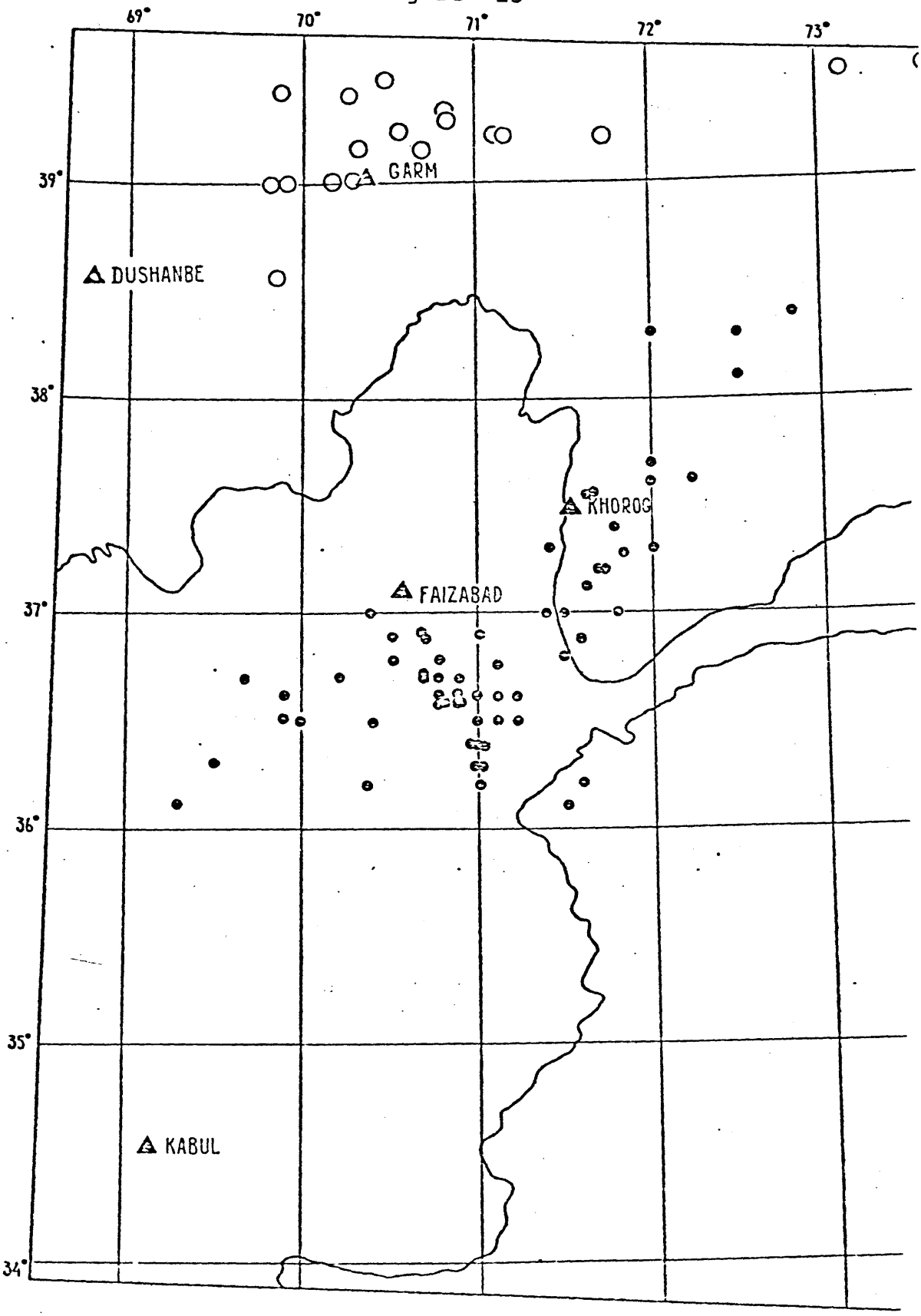
69°
70°
71°
72°
73°
39°
38°
37°
36°
35°
34°
GARM
DUSHANBE
KHOROG
FAIZABAD
KABUL

Figure 26

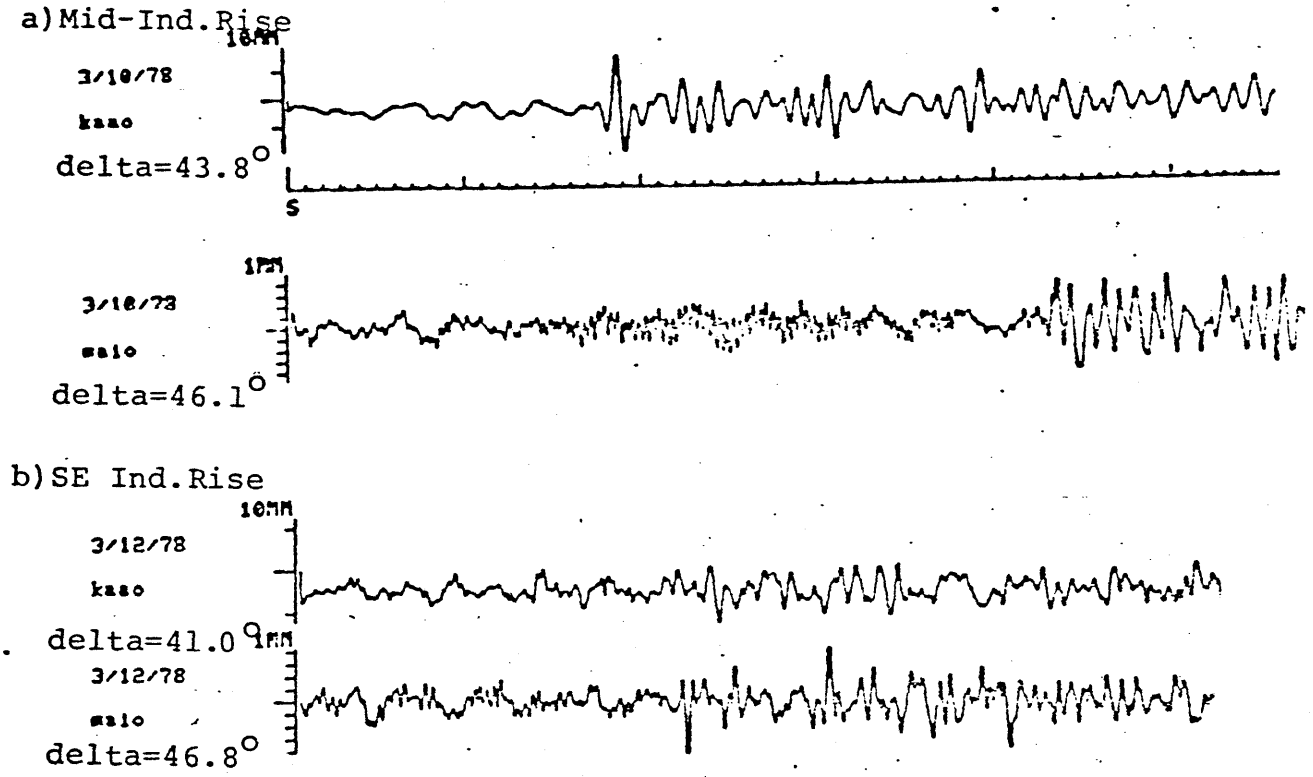
a) Mid-Ind. Rise
10mm
3/10/78
kaao
delta=43.8°
S
3/10/78
delta=46.1°
b) SE Ind. Rise
10mm
3/12/78
kaao
delta=41.0°
3/12/78
delta=46.8°

Figure 27

EVENTS FROM CRETE